OUKA
Osaka University Knowledge Archive

Title	Direct Optical Switching Code Division Multiple Access Systems for Fiber-Optic Radio Networks
Author(s)	Park, Sang-Jo
Citation	大阪大学, 1999, 博士論文
Version Type	VoR
URL	https://doi.org/10.11501/3155405
rights	
Note	

Osaka University Knowledge Archive : OUKA

https://ir.library.osaka-u.ac.jp/

Osaka University

Direct Optical Switching Code Division Multiple Access Systems for Fiber-Optic Radio Networks

Sang-Jo Park

Osaka University

January 1999

Acknowledgments

The research described in this thesis has been carried out by the author during his Ph. D course at the Department of Communications Engineering, Graduated School of Engineering, Osaka University.

The author would like to express his sincere gratitude to his supervisor, Professor Shozo Komaki, for giving the author an opportunity to study as a Ph. D student and for his academic advice, encouragement, and various supports throughout this research.

The author gives his appreciation to Professor Norihiko Morinaga and Associate Professor Masayuki Matsumoto for their readings and valuable criticisms on the whole contents of this thesis.

The author gives his appreciation to Professor Hajime Maeda, Professor Hiromasa Ikeda, Professor Hiroshi Motoda, Professor Yuji Kodama and Professor Toshiyuki Shiozawa of Graduated School of Engineering, Osaka University for their valuable comments on this research.

The author wants to appreciate Assistant Professor Minoru Okada and all members of Komaki Laboratory, especially Mr. Yozo Shoji, Mr. Masahiro Nishi and Mr. Satoshi Kajiya of Mitsubishi Co. Ltd. for their valuable comments on this study.

The author also thanks Associate Professor Katsutoshi Tsukamoto for his academic guidance and detailed comments throughout this study.

Without the scholarship from Ministry of Education, Science Research and Culture, Japan and the financial support from Electronics and Telecommunications Research Institute(ETRI), Korea, this research could not have carried out. The author gives his appreciation to both for their special helps as well as financial supports.

The author thanks Dr. Manseop Lee, Dr. Kanghee Yoo, Mr. Seongsoo Kang and Mr. Changoo Lee of ETRI, Korea for their encouragements and supports.

Finally, the author expresses his appreciation to his parents, brothers, wife Munsuk Lim, daughter Solah and son Junwhan for their endless loves and encouragements.

Preface

Recently, the international mobile telecommunication for the 2000s(IMT-2000), wireless asynchronous transfer mode(ATM) systems and future cable television(CATV) systems have been extensively developed to satisfy the increasing demand for the multimedia communications including voices, video-on-demands, high speed data and so on. In addition, future mobile communications providing multimedia services should have two important capabilities: one is the globally enhanced seamless connection capability among a huge number of cells, and the other is the flexibility and universality for diversified and various radio signal formats. However, broadband multimedia communications will need a lot of frequency resources and the microcellular/picocellular technology has many problems including the signal transfer among many microcells.

To solve these problems, fiber-optic radio networks have been studied. As an effective multiple access method for various types of radio signals over an fiber-optic link, the optical code division multiple access(CDMA) method will be a strong candidate. The optical CDMA methods have been studied mainly for digital optical local area network(LAN)s.

This thesis proposes optical CDMA methods for fiber-optic radio highway networks that can operate for such future mobile communications and is organized by the following six chapters.

Chapter 1 describes the purposes of this thesis in conjunction with the backgrounds.

Chapter 2 describes optical code division multiple access methods for fiber-optic radio networks. Multiple access methods for fiber-optic radio networks and conventional optical CDMA methods are described. We discuss the necessity for a new type of the optical CDMA method for fiber-optic radio highway networks.

Chapter 3 describes the concept of cable-to-the-air (CATA) system and the principle of the direct optical switching(DOS) CDMA for fiber-optic radio networks including CATA

systems. We propose two types of bus connection methods, the optical coupler connection and the optical switch connection where an optical switch is used not only to spread the spectrum of optical signals but also to launch them into the fiber-optic bus link. Then, in two types of DOS-CDMA CATA systems, we theoretically analyze the carrier-to-interference-plus-noise power ratio(CINR)s of regenerated radio signals. The results show that, in the optical switch connection system, by introducing the additional optical gain at each radio base station, the CINR's for all radio base stations and the connected number of radio base stations can be improved compared with the optical coupler connection system.

Chapter 4 proposes the optical polarity reversing correlator(OPRC) for the DOS-CDMA scheme in order to apply PN codes that are usually used in CDMA radio systems. The CINR of the regenerated radio signal is theoretically analyzed. The results show that, for small average transmitted optical powers, the OPRC using Gold codes can more improve the number of maximum connected radio base stations than the unipolar type correlator using prime codes.

Chapter 5 proposes the reversing optical intensity(ROI) CDMA where the spectrum spreading is performed for all intervals of a PN code in order to increase the received optical power at the receiver and have the flexibility for conventional CDMA radio systems. We apply the ROI-CDMA routing scheme to conventional CDMA radio systems in order to route code division multiplexing(CDM) signals to the control station. The CINR of the regenerated radio signal is theoretically analyzed. As a result, the CINR can be more improved by increasing the code sequence length at the ROI-CDMA transmitter than that in the radio highway using the electrical CDMA and intensity modulation(IM) method.

Chapter 6 summarizes the results obtained from this study.

The work summarized in this thesis has been carried out by the author during his Ph. D course at the Department of Communications Engineering, Graduated School of Engineering, Osaka University, during 1995-1999.

Sang-Jo Park

Osaka, Japan
January 1999

Contents

List of Figures

Chapter 1

Introduction

Recently, the international mobile telecommunication for the 2000s(IMT-2000) [1] , wireless asynchronous transfer mode(ATM) systems [2] and future cable television(CATV) systems [3] have been extensively developed to satisfy the increasing demands for the multimedia communications including voices, video-on-demands, high speed data and so on. To satisfy these demands, we need to realize broadband transmissions, and the fiber optic systems have been introduced into trunk networks as one of the solutions. On the other hand, radio access links for broadband communications have a variety of features such as the portability of set-top box (STB)es and the flexible construction of access links [4]. The wired local loop system will be used for the radio signal delivery to construct indoor wireless networks. However, mobile wireless communications or mobile computings should be operated as anytime and anywhere as possible, so we must provide the same communication environments both for insides such as in-houses, offices, in-shops and so on, and for outsides such as streets, in-cars, stations and so on. In addition, future mobile communications providing multimedia services should have two important capabilities: one is the globally enhanced seamless connection capability among a huge number of cells, and the other is the flexibility and universality for diversified and various radio signal formats. Wide-band data transmissions need a lot of frequency resources, thus microcellular systems have been proposed [5]. However, the microcellular technology has many problems including the signal transfer and switching among many microcells and the installation of new radio base station(RBS)s.

To solve these problems, fiber-optic microcellular systems have been proposed and

studied [6]-[7]. In this system, microcells in wide area are connected by optical fibers and radio signals are transmitted over fiber-optic links among microcells and a control station(CS). This system can simultaneously open radio free spaces among several users and CS's according to user's demand. We have called this space as "Virtual radio free space" and have proposed "Fiber-optic radio networks" [8]-[9]. This network can operate for any types of air interfaces, and needs no restoration of RBS's to start any new services for global area. Moreover, this network can realize the universal capability and flexibility for various types of air interfaces such as microcelluar radio systems, fiber-to-the-air (FTTA) systems, B-ISDN ATM based high speed radio distributions and so on. A RBS is only equipped with an electric-to-optic(E/O) and an optic-to-electric(O/E) converter, and all of complicated functions such as the RF modulation/ demodulation and the spectrum delivery switching are installed at the CS.

We investigate the configuration of fiber-optic radio highway networks. Conventionally, a single star configuration has been mainly investigated because of its simplicity and high reliability. However, a problem in this configuration is the enormous investment for the construction of many fiber-optic links. Moreover, we should consider robust and flexible architecture as well as cost-efficient configuration for fiber-optic radio highway networks. Reference [10] has reported that the bus type optical link or the passive double star link provides not only lower cost implementation, but also much more robust and flexible configuration than the star type optical link. So we adopt the bus type optical link as a configuration of fiber-optic radio highway networks [6][13]. Therefore, we should consider multiple access methods for fiber-optic radio highway networks. As a multiple access method for fiber-optic radio highway networks, subcarrier division multiple access(SCMA) methods [6][11] and time division multiple access(TDMA) methods [12]-[13] have often been discussed. The SCMA method excels in simplicity and flexibility, however, each cell needs a different radio frequency and optical signal beat noises severely deteriorate the carrier-to-noise ratio(CNR) at the CS if there are no strict controls of optical wavelengths of laser diodes connected to fiber-optic at each RBS. Reference [14] investigates the reduction of optical signal beat noises in the SCM/ wavelength division multiplexing(WDM) network, however the spectrum spreading technique has not been investigated. On the other hand, in the TDMA method no optical signal beat noise

arises and a radio frequency can be reused among several microcells, however, this method needs the time synchronization of the whole system. In the downlink of fiber-optic radio highway networks, for example, the radio or video distribution can be provided by the conventional multiplexing method such as the SCMA method. On the other hand, the uplink traffic is not so large in spite of many potential subscribers, but there exist various types of radio signals which have different frequencies and different multiple access methods. Thus, the code division multiple access(CDMA) method will be a strong candidate as a multiple access method for the uplink of fiber-optic radio networks because of its asynchronous access property, flexibility and transparency for various radio air interfaces. As CDMA methods that are applied for fiber-optic radio highway networks, there are two methods : one is the electrical CDMA and intensity modulated(IM) method [15] where radio signals are spectrum-spread and their correlations are performed in the electrical domain. Another is the optical CDMA method where radio signals are spectrum-spread and their correlations are performed in the optical domain. Out of two CDMA methods for fiber-optic radio networks, the optical CDMA method is more suitable than the conventional electrical CDMA and IM method because radio signals are multiplexed in the optical domain and high processing gains can be gained with ease by using the broad bandwidth of optical devices.

Up to this time, various optical CDMA methods have been studied mainly for digital optical local area network(LAN)s. Optical CDMA methods such as using fiber delay lines [16]-[20], optical phase masks [21]-[22] and coherent optical phase modulations [23]-[25] have been proposed and studied. In the optical CDMA method using fiber delay lines, the encoding and the decoding are performed by delaying optical pulses in the time domain. In the optical CDMA method using optical phase masks, the spectral encoding and the decoding are performed by phase-modulating optical pulses in the optical frequency domain. However, these methods can not be applied for multiplexing radio signals for fiber-optic radio networks. Furthermore, these methods have no flexibility in assigning code sequences. In the optical CDMA method using coherent optical phase modulations, its correlators are very complicated and need very fine narrowband optical filters that are very sensitive to temperature changes. On the other hand, the optical CDMA using optical disk patterns [26] has been proposed, however in this method the

assigning code sequences is not flexible and the application to radio signals has not been taken.

Therefore, we investigate optical CDMA methods for fiber-optic radio highway networks from the view points of the flexibility in assigning code sequences and the use of the optical intensity modulation. In this thesis, we investigate the direct optical switching (DOS)-CDMA scheme as a multiple access for fiber-optic radio networks [27]-[30], where a radio signal is converted into an optical intensity-modulated (IM) signal and the multiplexing is performed with randomizing positions of optical pulses by driving directly an OSW on-off switchings with a code sequence. So any types of radio signal can be converted into optical intensity-modulating (IM) / CDMA signals. We apply the concept of fiber-optic radio highway networks to the CATV system and firstly call it cable-to-the-air (CATA) system [27]. The configuration of the DOS-CDMA CATA system is proposed by using the optical coupler(OC) connection and the optical switch(OSW) connection and their performances using prime codes are theoretically analyzed [29][30].

As an optical orthogonal code, the prime code that is applied to obtain a desired process gain in optical CDMA methods [16]-[20], suffers a limit in the number of distinct code sequences, which results in the limitation of the number of radio base stations connected to fiber-optic radio networks. Besides in fiber-optic radio networks using DOS-CDMA with prime codes, the optical power efficiency is low because the pulse duty of a prime code is quite low. Therefore, we should consider a new type of correlator for DOS-CDMA method to which pseudo noise(PN) codes such as Maximal length codes and Gold codes can be applied because those codes are usually used in radio system and generally superior in the number of distinct code sequences compared with prime codes. For digital networks using optical CDMA methods, sequence inversion keyed(SIK) direct sequence(DS) CDMA methods that have been proposed in Refs.[31]-[32], require specially balanced PN codes. In order to allow the use of any unbalanced PN codes, the power splitting ratio of the power divider at the optical correlator has been controlled [33], and the transmission of two channels using two wavelengths or two orthogonal polarizations has been proposed [34]. In SIK-CDMA methods, however, binary digital data are encoded and transmitted with the positive polarity and the negative polarity of bipolar codes, thereby their correlators at the receiver can not be applied to DOS-CDMA signals

that are converted from radio signals by the on-off switching CDMA method.

In this thesis, we newly propose the optical polarity-reversing correlator(OPRC) for DOS-CDMA radio highway networks using PN codes [35]-[39]. In DOS-CDMA methods, as the optical power is zero for the interval of zero parts in prime codes or negative polarity parts in PN codes, the received optical power at the receiver is less than the laser power at the RBS. Moreover, the optical CDMA using all intervals of PN codes for fiber-optic radio networks is needed in order to have the flexibility for conventional CDMA radio systems. In this thesis, we newly propose the reversing optical intensity(ROI) CDMA method where the spectrum spreading is performed for all intervals of a PN code [40]-[41]. We apply the ROI-CDMA routing scheme to conventional CDMA radio systems to route CDM signals to the routing destination CS [41]. In the proposed networks, we theoretically analyze the carrier-to-interference-plus-noise power ratio(CINR)s of regenerated radio signals because the noise power is the important factor in fiber-optic radio networks, however in conventional CDMA radio systems the carrier-to-interference-power ratio(CIR) is analyzed.

In this thesis, we treat the following five chapters :

Chapter 2 describes optical code division multiple access methods for fiber-optic radio networks. Multiple access methods for fiber-optic radio networks and the conventional optical CDMA methods are described. The necessity for a new type of the optical CDMA method for fiber-optic radio highway networks is discussed.

Chapter 3 describes the concept of cable-to-the-air (CATA) system and the principle of the direct optical switching CDMA for fiber-optic radio networks including CATA systems. We propose two types of bus connection methods, the optical coupler connection and the optical switch connection where an optical switch is used not only to spread the spectrum of optical signals but also to launch them into the fiber-optic bus link. Then, in two types of DOS-CDMA CATA systems, we theoretically analyze the carrier-to-interference-plus-noise power ratio(CINR)s of regenerated radio signals. The results show that by introducing the additional optical gain at each radio base station, the CINR's for all radio base stations and the connected number of radio base stations can be improved in the optical switch connection system compared with the optical coupler connection system.

Chapter 4 proposes the optical polarity reversing correlator(OPRC) for the DOS-CDMA scheme in order to apply PN codes that are usually used in CDMA radio systems. The CINR of the regenerated radio signal is theoretically analyzed. The results show that, for small average transmitted optical powers, the OPRC using Gold codes can more improve the number of maximum connected radio base stations than the unipolar type correlator using prime codes.

Chapter 5 proposes the reversing optical intensity(ROI) CDMA where the spectrum spreading is performed for all intervals of a PN code in order to increase the received optical power at the receiver and have the flexibility for conventional CDMA radio systems. We apply the ROI-CDMA routing scheme to conventional CDMA radio systems to route code division multiplexing(CDM) signals to the routing destination control station. The CINR of the regenerated radio signal is theoretically analyzed. As a result, the CINR can be more improved by increasing the code sequence length at the ROI-CDMA transmitter than that in the radio highway using the electrical CDMA and intensity modulation(IM) method.

Chapter 6 summarizes the results obtained from this study.

Chapter 2
Optical Code Division Multiple Access Method for Fiber-Optic Radio Networks

2.1 Introduction

A bus type optical link or a passive double star link is preferable for fiber-optic radio highway networks because it provides more the reduction in conduits and optical fiber lengths as well as more robust and flexible interconnection architectures than a star link [10]. Therefore, we should consider effective multiple access methods for various types of radio signals over a fiber-optic link. The uplink traffic in fiber-optic radio networks is not so large in spite of many potential subscribers, but there exist various types of radio signals which have different frequencies and different multiple access methods. Thus, the CDMA method will be a stronger candidate as a multiple access method for the uplink of fiber-optic radio networks because of its asynchronous access property, flexibility and transparency for various radio air interfaces than SCMA methods [6][11] and TDMA methods [12]-[13].

In radio highway networks using the electrical CDMA method and intensity modulation(IM) method [12], radio signals are spectrum-spread and their correlations are performed in the electrical domain. As a CDMA method for fiber-optic radio highway networks, the optical CDMA method is more suitable than the electrical CDMA method in order to multiplex radio signals in the optical domain and to gain high processing gains.

Up to this time, various optical CDMA methods using such as optical pulse codings using

fiber delay lines [16]-[19] and optical phase masks [21]-[22], and coherent optical phase modulations [23]-[25] have been studied mainly for digital signals in the LAN. The optical CDMA method using optical pulse codings can not be applied to analog radio signals, because their CDMA transmitters and correlators are based on optical pulses. In the optical CDMA method using coherent optical phase modulations, its correlators have considerable complexities. On the other hand, the optical CDMA using optical disk patterns [26] has been proposed, however in this method the assigning code sequences is not flexible and the application to radio signals has not been taken.

So we investigate optical CDMA methods for the uplink of fiber-optic radio highway networks from the view points of the flexibility in assigning code sequences and the use of the optical intensity modulation.

2.2 Multiple Access Method for Fiber-Optic Radio Networks

Recently, wide-band data transmissions need a lot of frequency resources and microcellular systems have been proposed [5]. However, the microcellular technology has many problems including the signal transfer and switching among many microcells and the installation of new radio base station(RBS)s. To solve these problems, fiber-optic microcellular systems have been proposed and studied [6]-[7]. In this system, microcells in wide area are connected by optical fibers and radio signals are transmitted over fiber-optic links among microcells and a control station(CS). This system can simultaneously open radio free spaces among several users and CS's according to the user's demand. We have called this space as "Virtual radio free space" and have proposed "Fiber-optic radio network" [8]-[9]. This network can operate for any types of air interfaces, and needs no restoration of radio base station(RBS)s to start any new services for global area. Figure 2.1 illustrates the concept of fiber-optic radio networks which can realize the universal capability and flexibility for various types of air interfaces such as microcelluar radio systems, fiber-to-the-air (FTTA) systems, B-ISDN ATM based high speed radio distribution systems and so on. A RBS is only equipped with an electric-to-optic(E/O) and an optic-to-electric(O/E) converter, and all of complicated functions such as the RF modulation/

demodulation and the spectrum delivery switching are installed at the CS.

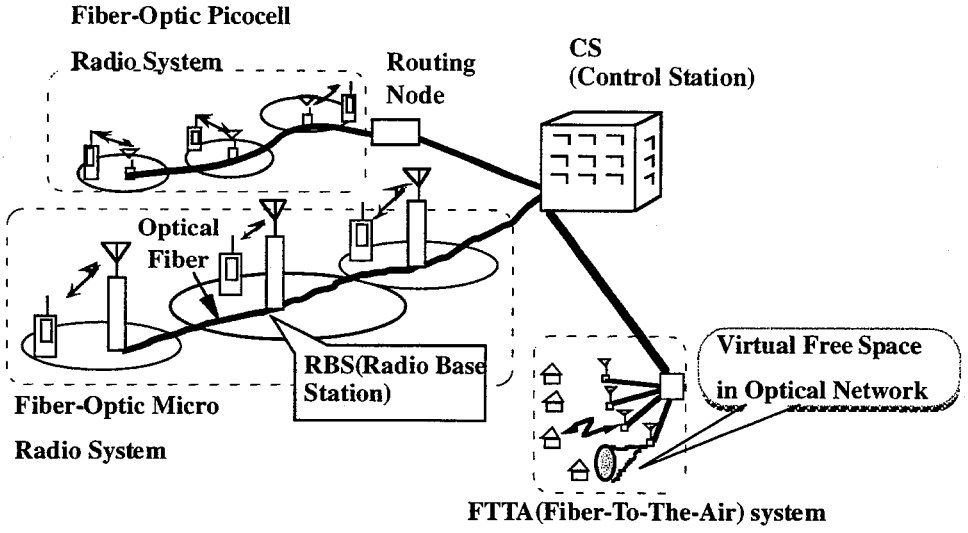

Fig.2.1 Concept of fiber-optic radio networks.

We investigate the configuration of fiber-optic radio highway networks. Conventionally, a single star configuration has been mainly studied because of its simplicity and high reliability. However, a problem in this configuration is the enormous investment for the construction of many fiber-optic links. Moreover, we should consider robust and flexible architecture as well as cost-efficient configuration for fiber-optic radio highway networks. Reference [10] has reported that the bus type optical link or the passive double star link provides not only lower cost implementation, but also much more robust and flexible configuration than the star type optical link. So we adopt the bus type optical link as a configuration of fiber-optic radio highway networks [6][13]. Therefore, we should consider multiple access methods for fiber-optic radio highway networks. As a multiple access method for fiber-optic radio highway networks, SCMA methods [6][11] and TDMA methods [12]-[13] have often been discussed. The SCMA method exceeds in simplicity and flexibility, however, each cell needs a different radio frequency and optical signal beat noises severely deteriorate the carrier-to-noise ratio(CNR) at the CS if there are no strict controls of optical wavelengths of laser diodes connected to the fiber-optic link at each RBS. Reference [14] investigates the reduction of optical signal beat noises in the SCM/ wavelength division multiplexing(WDM) network, however the spectrum spreading technique

has not been investigated. On the other hand, in the TDMA method no optical beat noises arise and a radio frequency can be reused among several microcells, however, this method needs the time synchronization of the whole systems. In the downlink of fiber-optic radio highway networks, for example, the radio or video distribution can be provided by the conventional multiplexing method such as the SCMA method. On the other hand, the uplink traffic is not so large in spite of many potential subscribers, but there exist various types of radio signals which have different frequencies and different multiple access methods. Thus, the CDMA method will be a stronger candidate as a multiple access method for the uplink of fiber-optic radio networks because of its asynchronous access property, flexibility and transparency for various radio air interfaces than SCMA methods [6][11] and TDMA methods [12]-[13]. Table 2.1 illustrates the characteristics of multiple access methods for fiber-optic radio highway networks.

Table 2.1 Characteristics of multiple access methods for fiber-optic radio highway networks.

Multiple access method	**Configuration**	**Characteristics**
Subcarrier division multiple access (SCMA)	use frequency division multiplexed RF signals	o simple and flexible x each cell needs different radio frequency
Time division multiple access (TDMA)	timewise sampled using optical switch	o radio frequency can be reused among cells x need time synchronization of whole system
Wavelength division multiple access (WDMA)	use different optical wavelengths	x difficult to control optical wavelengths

2.3 Optical Code Division Multiple Access Method

As the CDMA methods that are applied for fiber-optic radio highway networks, there are two methods : one is the electrical CDMA and IM method [15] where radio signals are spectrum-spread in the electrical domain and converted into IM signals at the laser diode(LD), and their correlations are performed in the electrical domain after the photodetection at the photodetector(PD) as shown in Fig.2.2.

Another is the optical CDMA method where radio signals are spectrum-spread and their correlations are performed in the optical domain. Out of two CDMA methods for fiber-optic radio highway networks, the optical CDMA method is more suitable than the conventional electrical CDMA method because radio signals are multiplexed in optical domain and high processing gains can be gained with ease by using the broad bandwidth of optical devices.

Up to this time, various optical CDMA methods have been studied mainly for digital optical LAN's. Optical CDMA methods such as using fiber delay lines [16]-[20], optical phase masks [21]-[22] and coherent optical phase modulations [23]-[25] have been proposed and studied.

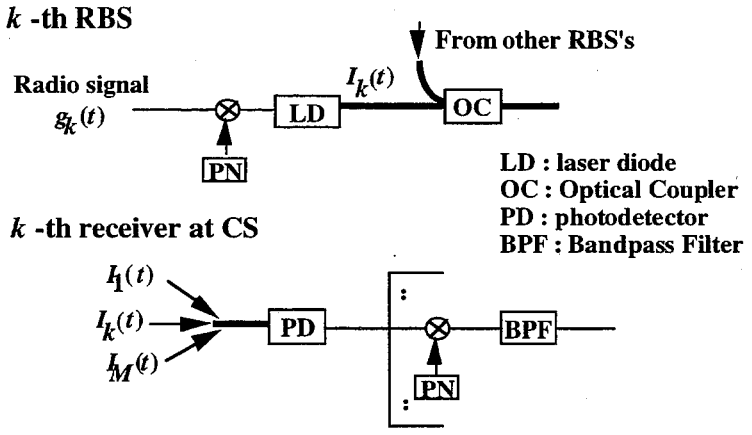

Fig.2.2 Configuration of the electrical CDMA and IM method.

Fig. 2.3 illustrates examples of conventional optical CDMA methods. In the optical CDMA method using fiber delay lines, the encoding and the decoding are performed by delaying optical pulses in the time domain. In the optical CDMA method using optical phase masks, the spectral encoding and the decoding are performed by phase-modulating optical pulses in the domain of optical frequency. However, these methods can not be applied for multiplexing radio signals for fiber-optic radio highway networks. Furthermore, these methods have no flexibility in assigning code sequences. In the optical CDMA methods using coherent optical phase modulations, its correlators are very complicated and need very fine narrowband optical filters that are very sensitive to temperature changes. On the other hand, the optical CDMA using optical disk patterns has been proposed [26], however in this method, the assigning code sequences is not flexible and the application to radio signals has not been taken.

Therefore, we investigate optical CDMA methods for fiber-optic radio highway networks from the view points of the flexibility in assigning code sequences and the optical CDMA using the optical intensity modulation.

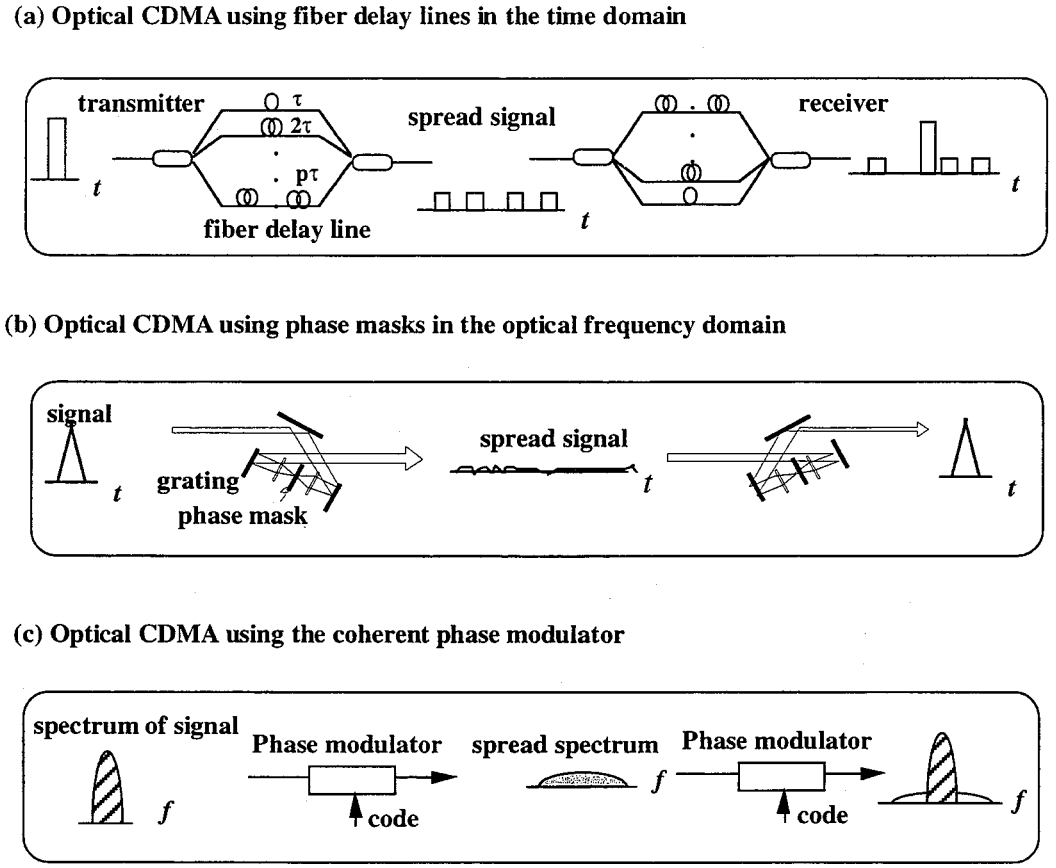

Fig. 2.3 Examples of conventional optical CDMA methods.

2.4 Concluding Remarks

This chapter has described the various types of multiple access methods for fiber-optic radio networks and performed the comparison of these methods. Among them, the CDMA method is suitable for the uplink of fiber-optic radio networks. Also we have described the conventional optical CDMA methods and discussed the necessity for a new type of the optical CDMA method for the uplink of fiber-optic radio highway networks.

Chapter 3

Fiber-Optic Radio Networks Using Direct Optical Switching(DOS) CDMA And Its Performance Analysis

3.1 Introduction

A future CATV system [3] needs a broadband transmission link to offer interactive multimedia services including voices, high quality videos, video-on-demands, high speed data and so on. In addition, future mobile communications providing multimedia services should have two important capabilities: one is the globally enhanced seamless connection capability among a huge number of cell, and the other is the flexibility and universality for diversified and various radio signal formats.

To solve above problems, we apply the concept of the FTTA system to the CATV system. We first call such a system cable-to-the-air (CATA) system [27]. The CATA system is a broadband wireless local loop, but by using progressive microwave/millimeter wave photonics techniques, radio signals from subscribers are transmitted among radio base stations (RBS) and a head end (HE) with radio signal formats kept over an optical fiber. Figure 3.1 illustrates the concept of the CATA system, where radio signals are encapsulated into the envelope of optical signal through fiber-optic links. Since a RBS is only equipped with an E/O converter and an O/E converter, and all of complicated functions such as the RF modulation /demodulation and

the spectrum delivery switching are performed at the HE, the CATA system can accommodate various types of radio interfaces such as mobile communications, video broadcastings, in-house radio networks and so on, and moreover it can provide the same wireless communication environments for both indoor and outdoor. The CATA system also has a great flexibility for any changes or additions of radio services. For example, at first, this system provides a video-on-demand (VOD) service, and later it can immediately offer any new mobile communication services or new video standards with no restoration of new set-top box(STB)es and only with additional equipments at the HE.

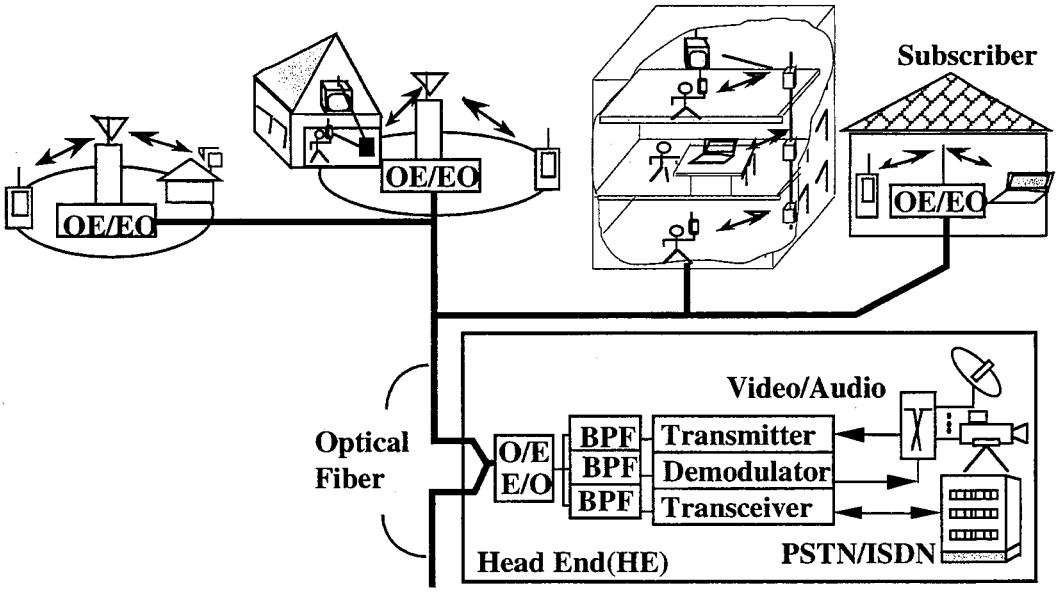

Fig. 3.1 Concept of the CATA system.

In the downlink of CATA system, for example, the radio or video distribution can be provided by conventional multiplexing methods such as SCMA methods. On the other hand, the uplink traffic is not so large in spite of many potential subscribers, but there exist various types of radio signals which have different frequencies or different multiple access methods. Thus, the optical CDMA method will be more suitable as a multiple access in the optical link because of its asynchronous access property, greater flexibility and transparency for various radio air

interfaces than the SCMA method and the TDMA method.

In this chapter, we investigate the optical CDMA method for the uplink of fiber-optic radio networks including CATA systems from the view points of the flexibility in assigning code sequences and the use of the optical intensity modulation. The direct optical switching (DOS)-CDMA scheme is investigated as a multiple access for fiber-optic radio networks [27]-[30]. The proposed DOS-CDMA scheme can be performed only with an optical switch(OSW) at the transmitter and also an OSW, a photodetector(PD), and an electrical bandpass filter(BPF) at the receiver. So any types of radio signals can be converted into optical intensity-modulating (IM) / CDMA signals. When applying DOS-CDMA scheme for a bus type optic-fiber link, an OSW spreading the signal spectrum can be also used to launch them into the fiber link. In the DOS-CDMA scheme, the multiplexing is performed by randomizing positions of optical pulses by driving an OSW with a pseudo random code sequence. This is quite different from the random access discrete address (RADA) scheme using the quantized pulse position modulation (PPM) [42].

We propose the configuration of DOS-CDMA CATA system by using the optical coupler(OC) and the optical switch(OSW) connections and theoretically analyze their performances. The remainders of this chapter are composed as followings: In Sect. 3.2, we describe the principle of DOS-CDMA scheme and the configuration of the DOS-CDMA CATA system that is composed of two types of bus connection methods, the optical coupler(OC) connection type and the OSW connection type. In the OSW connection type CATA system, an OSW is used not only to spread the spectrum of optical signals but also to launch them into the fiber-optic bus link. In Sect. 3.3, we theoretically analyze the carrier to interference-plus-noise ratio (CINR)s of the radio signals regenerated at the HE for two types of bus connection methods considering the chip pulse erasure at the OSW. In Sect. 3.4, some numerical results are discussed and compared between two types of bus connection methods.

3.2 Direct Optical Switching(DOS) CDMA Cable-To-The-Air(CATA) System

3.2.1 Principle of DOS-CDMA Method

The DOS-CDMA scheme uses the on-off type switching spectral spreading. Each radio signal received at each RBS is transmitted to a HE by analog type optical pulse amplitude modulation(PAM) scheme, and the multiple access among many RBS's is performed by the DOS-CDMA scheme. The regeneration of radio signal is based on the bandpass natural sampling theory [13][43]. Figure 3.2 shows the system model of DOS-CDMA system to illustrate the principle of the DOS-CDMA process at the RBS transmitter and the correlating process at the HE receiver.

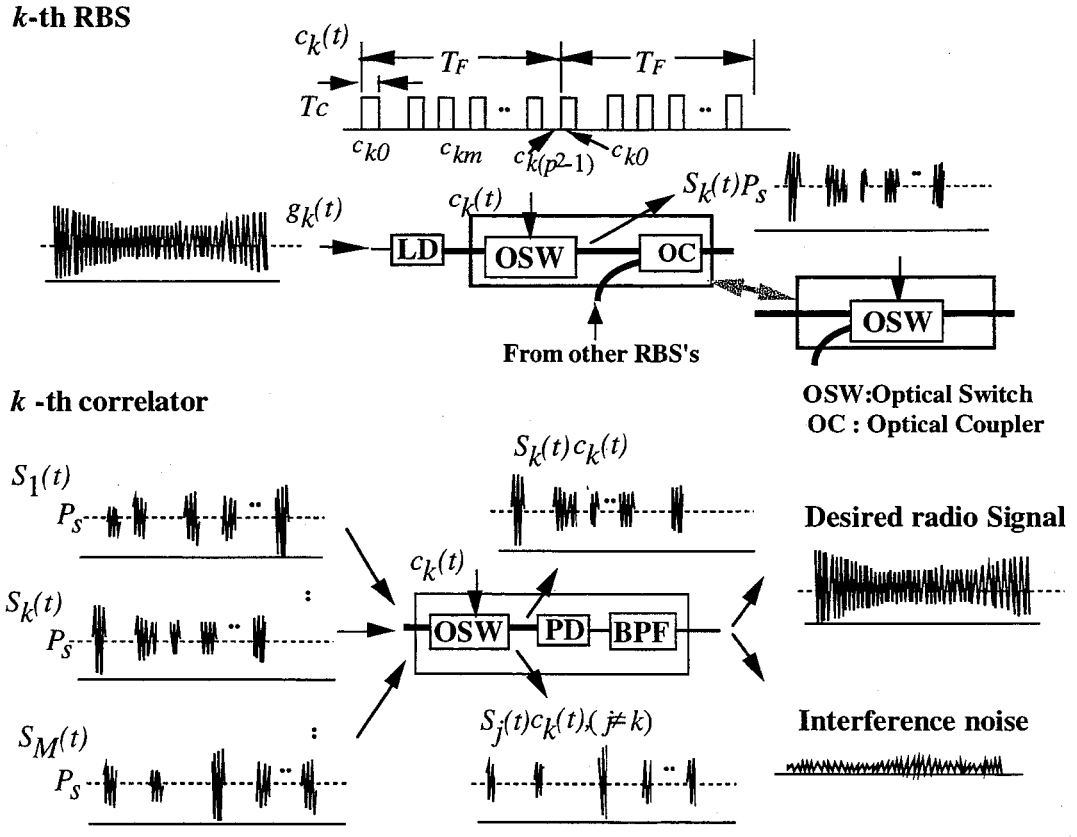

Fig. 3.2 Principle of the DOS-CDMA process.

At a RBS, a received radio signal is converted into an optical intensity-modulated (IM) signal by modulating LD directly and next sampled at an OSW, which is driven with a certain code sequence, $c_k(t)$, and the output signal of OSW is transmitted to a receiver through optical fiber. At the output of OSW in the transmitter, we can obtain optical PAM/IM signals whose pulses are positioned according to the code pattern of $c_k(t)$. At the receiver, many PAM/IM signals from many RBS's are correlated with the code sequence, $c_k(t)$, at an OSW, then directly detected at a PD and interpolated at a BPF to regenerate the desired radio signal. It is assumed that the code sequence, $c_k(t)$, matched with the one at the RBS is regenerated at the HE and the synchronization between two code sequences is taken. The radio signal which is contaminated by all other radio signals, is fed into a demodulator in order to obtain the information data.

The radio signal $g_k(t)$ at the k-th RBS is represented by

$$g_k(t)=\mathrm{Re}\left[a_k(t)e^{j2\pi f_{rf}t}\right], \tag{3.1}$$

where f_{rf} is radio frequency and $a_k(t)$ is the complex envelope with its bandwidth, B_{rf}. The optical on-off switching CDMA is performed at the OSW driven by a code sequence, $c_k(t)$, whose frame period and chip width are T_F(sec) and T_c respectively and its pulse amplitude is 1 or 0. The intensity of the optical PAM/IM signal at the output of the OSW is given by

$$P_k(t)=P_s\{1+g_k(t)\}c_k(t), \tag{3.2}$$

where P_s is the average transmitted optical power before optical switching.

The $P_k(t)$ is a bandpass natural sampled signal converted from a radio signal because an optical switching is a window-type sampling. Therefore, a radio signal can be conveyed by optical carrier with its signaling format kept and regenerated from the pulsed signals by the interpolation at a BPF if we choose sampling period of less than or equal to half of the inverse of radio signal bandwidth, $\leq 1/(2B_{rf})$ [43]. In the proposed DOS-CDMA system, since a pseudo random sequence is chosen as a code sequence which drives the OSW at the transmitter, the durations between optical pulses become various values according to the kind of code sequence, but each pulse is surely repeated with its frame period of T_F. Therefore, in order to regenerate the radio signal after interpolation, T_F of less than or equal to $1/(2B_{rf})$ should be chosen. From the viewpoint of simplicity, using T_F of much less than $1/(2B_{rf})$ is not effective, because a much faster speed for OSW is required. Hence, in this paper, T_F is set to be the maximum value, that

is, $1/(2B_{rf})$.

To improve the quality of the regenerated radio signal in DOS-CDMA system, a code sequence with the highest possible autocorrelation and the lowest possible cross-correlation has to be chosen. In the DOS-CDMA using optical IM/direct detection (DD) scheme, a uniphase code has to be used as a code sequence, while PN codes like maximum length or Gold code are used in conventional radio CDMA system. References [16]-[20] have reported that a prime code sequence is the best code as a uniphase orthogonal code which can provide the highest autocorrelation and the lowest cross-correlation of various orthogonal codes. So in the proposed DOS-CDMA system, the prime code sequence is employed as a spread spectrum (SS) code.

A set of prime codes has the preferable feature for IM/DD CDMA system that there are very few coincidences of 1's among code sequences. Prime codes with length, p^2, are derived from prime sequences obtained from a Galois field, $GF(p)$, where p is a prime number [46]. Table 3.1 shows an example of prime sequences and prime code sequences for a prime number p of 7. Each prime sequence element s_{mn} is obtained by the product of the corresponding m and n modulo p. Letting $c_m=(c_{m0},c_{m1},...,c_{mj},...,c_{m(p-1)})$ denote the m-th prime code sequence, a j-th code element, c_{mj}, is given by

$$c_{mj}=\begin{cases}1 & ; j=s_{mn}+np \\ 0 & ; \text{otherwise}\end{cases}. \tag{3.3}$$

In the DOS-CDMA scheme using prime codes, $T_F(=p^2T_c)$ is set to $1/(2B_{rf})$ in order to gain the largest code length, p^2, at the same switching speed of the OSW, thus the chip width, T_c, is given by T_F/p^2. When an OSW correlator is driven with the k-th prime code sequence, $c_k(t)$, at the receiver, the optical PAM/IM signal transmitted from the k-th RBS is extracted out of all CDMA signals. Then the output current of the PD is composed of a desired signal component, $S_k(t)$, interference components, $I(t)$, and additive noise components, $N(t)$. $S_k(t)$ and $I(t)$ are respectively given by

$$S_k(t)=\alpha P_r g_k(t)c_k(t), \tag{3.4}$$

$$I(t)=\alpha P_r \sum_{j=1,j\neq k}^{M} g_j(t)c_j(t)c_k(t), \tag{3.5}$$

where α, P_r and M are the responsivity of the PD, the average received optical power at the

correlator, and the total number of connected RBS's, respectively. Here, we derive the carrier to interference power ratio (CIR) in the DOS-CDMA system. We derive the power spectral density (PSD) of signal component, $S_k(t)$, by calculating the autocorrelation of $S_k(t)$ from Eq.(3.4). The PSD of $S_k(t)$, $S_k(f)$, is given by

$$S_k(f)=(\alpha P_r)^2\frac{1}{p^2}\left(1+\frac{1}{p}-\frac{1}{p^2}\right)\left\{G_k(f)+\frac{p-1}{p^2+p-1}\sum_{i=-\infty,i\neq 0}^{\infty}\mathrm{sinc}^2\left(\frac{\pi i}{p^2}\right)G_k\left(f-2iB_{rf}\right)\right\}, \tag{3.6}$$

where $G_k(f)$ is the power spectrum of $g_k(t)$ and $\mathrm{sinc}(x)$ is $\sin(x)/x$.

Table 3.1 Prime sequences and prime code sequences for prime number p=7.

Prime sequences for p=7

m	s_{m0}	s_{m1}	s_{m2}	s_{m3}	s_{m4}	s_{m5}	s_{m6}
0	0	0	0	0	0	0	0
1	0	1	2	3	4	5	6
2	0	2	4	6	1	3	5
3	0	3	6	2	5	1	4
4	0	4	1	5	2	6	3
5	0	5	3	1	6	4	2
6	0	6	5	4	3	2	1

Prime code sequences for p=7

m	c_{m0}	c_{m1}	c_{m2}	c_{m3}	c_{m4}	c_{m5}	c_{m6}
0	1000000	1000000	1000000	1000000	1000000	1000000	1000000
1	1000000	0100000	0010000	0001000	0000100	0000010	0000001
2	1000000	0010000	0000100	0000001	0100000	0001000	0000010
3	1000000	0001000	0000001	0010000	0000010	0100000	0000100
4	1000000	0000100	0100000	0000010	0010000	0000001	0001000
5	1000000	0000010	0001000	0100000	0000001	0000100	0010000
6	1000000	0000001	0000010	0000100	0001000	0010000	0100000

Figure 3.3 shows the normalized both-sides PSD of the signal component. The first three terms of $S_k(f)$ is the desired signal component around f_{rf} and $-f_{rf}$, and the other terms are the frequency shifted components caused by bandpass sampling. Images of these shifted components cause the distortion in the desired signal as the self-interference if they overlap over

the signal components as shown in Fig. 3.3 (a). We can perfectly remove the self-interference components by setting the value of the radio frequency f_{rf} at $(j+1/2)B_{rf}$ or j/T_c (j is an integer) as shown in Fig. 3.3 (b). Without such special values of f_{rf}, however, the self-interference component may not deteriorate the signal quality because its power is much low compared with that of the carrier signal component. We examine the carrier signal to self-interference power ratio (CSIR) and Figure 3.4 shows the some numerical results for the f_{rf} of 1.93GHz and B_{rf} of 900KHz. In the small value of p, the sinc function causes the up and down in CSIR, but as p increases, CSIR tends to be a saturated value of more than 30dB which is an enough value to obtain the radio signal quality in DOS-CDMA. As p increases, the saturated value of CSIR is determined by the relation between f_{rf} and B_{rf}. Therefore, in the following analysis, we will ignore the self-interference components.

From Eq. (3.6), the carrier power of the regenerated radio signal, C_0, is given by

$$C_0=(\alpha P_r)^2\frac{1}{p^2}\left(1+\frac{1}{p}-\frac{1}{p^2}\right). \tag{3.7}$$

Let σ_c^2 denote the average variance of the cross-correlation of the prime code. Then, the carrier to interference power ratio, CIR_0, is given by [16]-[20]

$$CIR_0=\frac{C_0}{I_0}=\frac{p^2}{\sigma_c^2(M-1)}. \tag{3.8}$$

Table 3.2 shows σ_c^2 for different values of prime number p calculated by using computer simulation. Table 3.2 shows that σ_c^2 is a little increased as p increases but has a saturated value of 0.329 for p=97.

Table 3.2 Average variance of the cross-correlation of the prime code.

p	σ_c^2
7	0.272
11	0.298
13	0.303
23	0.318
31	0.322
47	0.326
71	0.328
97	0.329

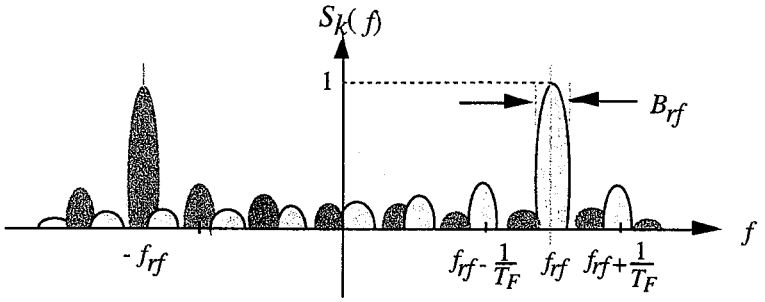

(a) Two components of desired signal and frequency shifted signal are overlapped.

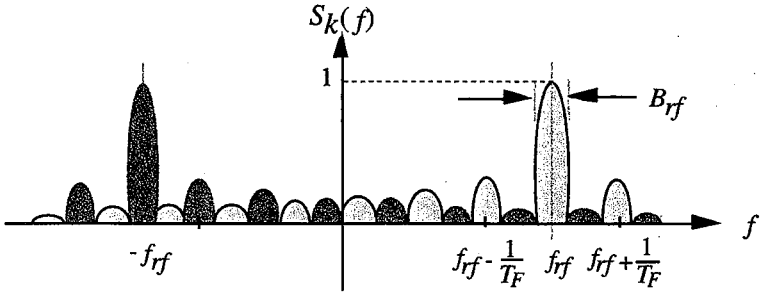

(b) Two components of desired signal and frequency shifted signal are not overlapped.

Fig. 3.3 Normalized both-side PSD of signal component.

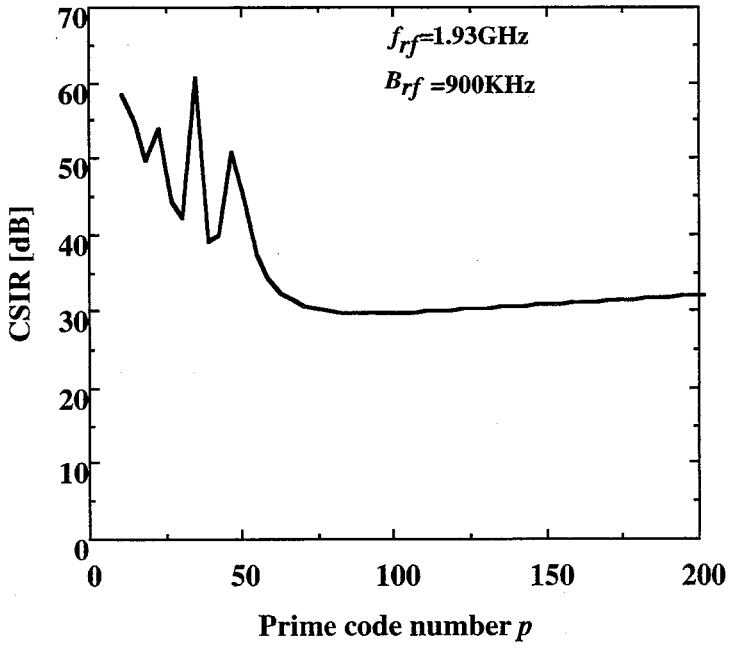

Fig. 3.4 Relationship between CSIR and prime code number p.

3.2.2 System Configuration

Figure 3.5 illustrates the configuration of the proposed DOS-CDMA CATA system. From the viewpoint of a cost effective configuration, we adopt a bus type fiber-optic link for CATA system. *M* radio zones are connected to the bus link, where the radio signals from radio terminals in each zone are multiplexed by the DOS-CDMA scheme and transmitted to the HE. The RBS in each zone equips only a LD, an optical switch (OSW) and an automatic gain controller (AGC).

As mentioned in sec. 3.2.1, after the direct-intensity-modulation of LD, the optical on-off switching spread spectrum (SS) is performed at the OSW, and in the bus type fiber link, many DOS-CDMA signals are multiplexed by CDMA. At the receiver, received optical powers are different among the received DOS-CDMA signals from *M* RBS's because the optical loss between each RBS and HE is different. Also, intensity modulation indices are different among the received CDMA signals because radio signal received by the RBS has various amplitudes due to fading and the different distance between terminals and a RBS. These differences cause the near-far problem in CDMA system. For this reason, a RBS is equipped with an automatic gain controller(AGC) to control the amplitude of a received radio signal in order to keep the optical modulation index constant at the LD, and also equipped with an OA to compensate optical loss between two RBS's.

At the HE, optical CDMA signals from RBS's are at first power-split into each of *M* receivers, then matched with one of different prime codes at each OSW correlator and detected at PD. Finally, the desired radio signal of each RBS is regenerated by the interpolation in BPF and then fed to a demodulator. In the conventional bus type fiber optic link, each node is usually connected to a bus link with a passive optical coupler (OC). In this case, there are the insertion loss and the coupling loss in a coupler. In the proposed DOS-CDMA CATA system where OC connection is used, the optical signal beat noise is caused by the interference between two lights arriving at the PD at the same time. On the other hand, an OSW is used not only to perform switching-spread-spectrum of the optical IM signal but also to launch them into the bus link. In

this chapter, a configuration of CATA system using the OC connection and the OSW connection is proposed. These two connection methods at a RBS are shown in Fig. 3.5. In the case of the OSW connection, when an IM/CDMA signal from RBS's that are further away from the HE arrives at the OSW of the those which are closer and transmitting their signals, the signal collision at the OSW of each RBS will cause the erasure of some chip pulses in DOS-CDMA signal as shown in Fig. 3.6. The detail will be discussed in Sect. 3.3.

3.3 Theoretical Analysis of Carrier-to-Interference-plus-Noise Ratio Performance

In this section, we theoretically analyze the carrier-to-interference-plus-noise power ratio(CINR)s of regenerated radio signals at the HE for both OC and OSW connections in the DOS-CDMA CATA system.

3.3.1 Optical Coupler Connection

At the k-th correlator, the average received optical power, P_{r_k}, can be written as

$$P_{r_k}=10\log_{10}P_s-k(L_f+L_{oc})+kG-10\log_{10}M+G_M[\text{dB}], \tag{3.9}$$

where L_{oc}[dB] , L_f[dB], G[dB] and G_M[dB] are the coupling loss plus the insertion loss of an OC, the fiber loss between RBS's, the gain of OA at the RBS and the gain of OA at the output of 1:M star coupler(SC), respectively [46]. It is assumed that an OA equipped at each RBS has the gain G of L_f+L_{oc} and G_M is equal to $10\log_{10}M$. From Eq.(3.9), therefore, P_{r_k} is given by

$$P_{r_k}=P_s\ (k=1,2,..,M), \tag{3.10}$$

At the HE, each correlator receives M optical signals with the same modulation index of 1 and the same received power, $P_r=P_s$, thereby the carrier power and the CINR of the regenerated radio signal are C_0 and CIR_0 given by Eqs.(3.7) and (3.8) in the case of $P_r=P_s$, respectively. At the output of BPF, we consider additive noise currents composed of relative intensity noise, shot noise, receiver thermal noise, beat noise among amplified spontaneous emissions (ASE) of an optical amplifier and optical signal, beat noise among ASE's and optical signal beat noise.

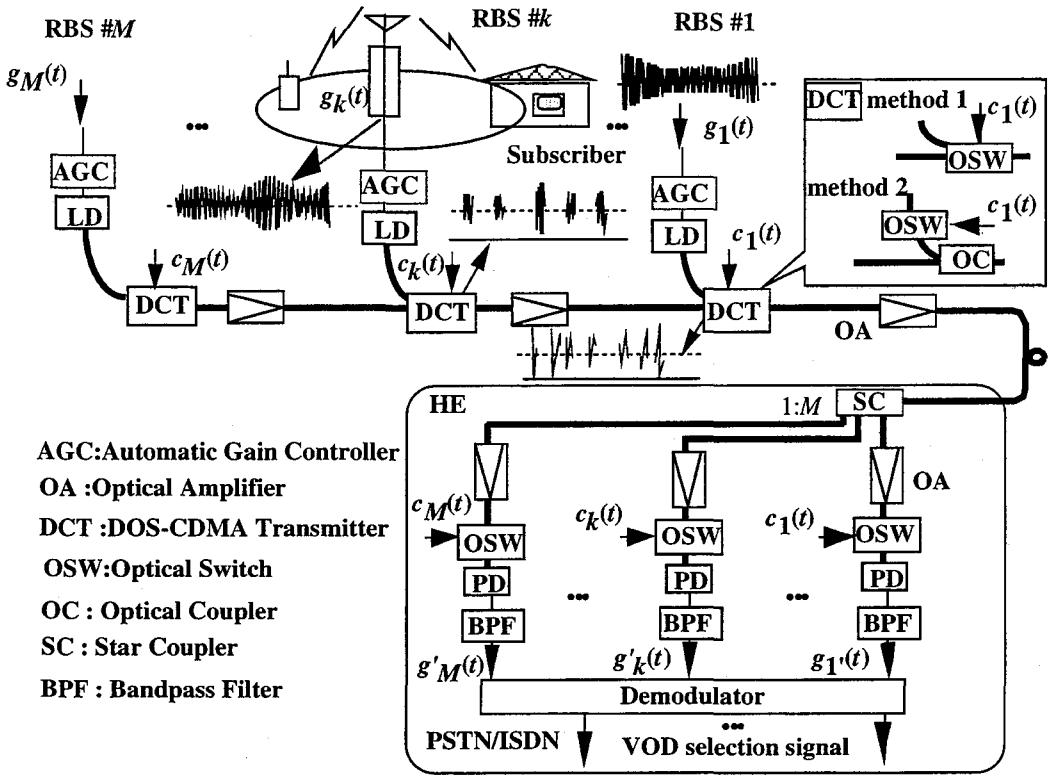

Fig. 3.5 Configuration of the proposed DOS-CDMA CATA system.

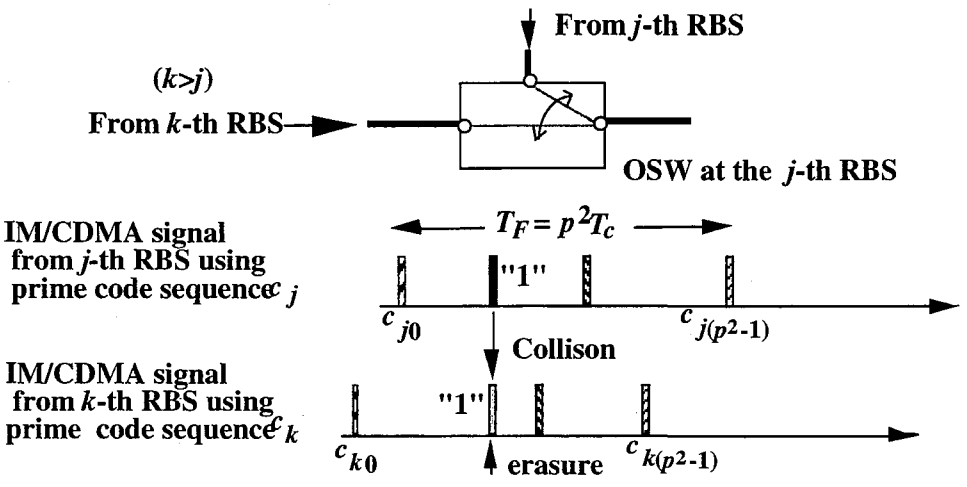

Fig. 3.6 Collision between two IM/CDMA signals.

Considering that the average number of coincidences of 1's between any prime code sequence pair in the interval of the code frame period, T_F, is one, that will be analyzed in Sect.3.3.2, the total noise power, N_c, is written by

$$N_c=N_{RIN}+N_{shot}+N_{th}+N_{s-sp}+N_{sp-sp}+\langle N_{s-s}\rangle \tag{3.11}$$

and each power is given by

$$N_{RIN}=\zeta_{RIN}\left(\frac{\alpha P_s}{p^2}\right)^2(p^2+M-1)B_{rf}, \tag{3.12}$$

$$N_{shot}=2e\left\{\left(\frac{\alpha P_s}{p^2}\right)(p+M-1)+\alpha M(N_{sp}+N_{sp_M})W\right\}B_{rf}, \tag{3.13}$$

$$N_{th}=\frac{4k_BT}{R_L}B_{rf}, \tag{3.14}$$

$$N_{s-sp}=4\alpha M(N_{sp}+N_{sp_M})\left(\frac{\alpha P_s}{p^2}\right)(p+M-1)B_{rf}, \tag{3.15}$$

$$N_{sp-sp}=2\alpha^2M^2\left(N_{sp}+N_{sp_M}\right)^2\left(W-f_{rf}\right), \tag{3.16}$$

where e, ζ_{RIN}, W, k_B, T and R_L are the electric charge, the PSD of the relative intensity noise, the bandwidth of optical filter at the HE, Boltzmann constant, the noise temperature and the load resistance, respectively. The PSD's of the ASE, N_{sp} and N_{sp_M}, are given by

$$N_{sp}=\frac{\eta_{sp}}{\eta_a}\cdot\frac{10^{G/10}-1}{10^{G/10}}h\nu, \tag{3.17}$$

$$N_{sp_M}=\frac{\eta_{sp}}{\eta_a}\cdot\frac{M-1}{M}h\nu, \tag{3.18}$$

respectively, where η_{sp}, η_a and $h\nu$ are the spontaneous emission factor, the quantum efficiency of the OA and the photon energy, respectively [6].

The optical signal beat noise, $\langle N_{s-s}\rangle$, is due to an interference between two optical carriers. In this analysis, it is assumed that the k-th RBS uses a LD with its center frequency of f_k and its single mode gaussian shaped spectrum, and also assumed that f_k is a random variable with a uniform probability density [15]. The PSD of the optical signal-signal beat noise is given

by

$$S_{s-s}(f)=\left(\frac{\alpha P_s}{p^2}\right)^2 \sum_{j=1}^{M}\sum_{\substack{k=1\\k\neq j}}^{M}\left\{\frac{1}{2\sigma\sqrt{2\pi}}e^{-\frac{(f-\Delta f_{jk})^2}{2\sigma^2}}+\frac{1}{2\sigma\sqrt{2\pi}}e^{-\frac{(f+\Delta f_{jk})^2}{2\sigma^2}}\right\}, \tag{3.19}$$

where

$$\Delta f_{jk}=f_j-f_k \tag{3.20}$$

$$\sigma=\Delta\nu/(2\log 2) \tag{3.21}$$

$$\Delta\nu=\sqrt{\Delta\nu_{LD}+\left(p^2 B_{rf}\right)^2} \tag{3.22}$$

where $\Delta\nu_{LD}$ is the full width half maximum(FWHM) of the LD, and $\Delta\nu$ is the FWHM after spread spectrum by prime codes with the prime number p. The PSD of the optical signal beat noise, $S_{s-s}(f)$, appears in the radio frequency band after the photodetection, but its frequency location depends on the frequency difference among LD's of M RBS's. So we treat its power N_{s-s} as a random variable and derive its average power $\langle N_{s-s}\rangle$. Assuming that optical carrier frequencies at RBS's, f_j ($j=1,2,\ldots, M$) are mutually independent random variables with its mean of f_0 and a uniform probability density function(PDF) in the range of $|f_j-f_0|<\frac{\Delta F}{2}$, then the power of optical signal beat noise falling in bandwidth B_{rf}, N_{s-s}, is given by

$$\begin{aligned}N_{s-s}&=\left(\int_{-f_{rf}-B_{rf}/2}^{-f_{rf}+B_{rf}/2}+\int_{f_{rf}-B_{rf}/2}^{f_{rf}+B_{rf}/2}\right)S_{s-s}(f)df\\&=\left(\frac{\alpha P_s}{p^2}\right)^2\sum_{j=1}^{M}\sum_{\substack{k=1,\\k\neq j}}^{M}\left[erfc\left\{\frac{-2(f_{rf}+\Delta f_{jk})-B_{rf}}{2\sqrt{2}\sigma}\right\}-erfc\left\{\frac{-2(f_{rf}+\Delta f_{jk})+B_{rf}}{2\sqrt{2}\sigma}\right\}\right.\\&\qquad\left.+erfc\left\{\frac{-2(f_{rf}-\Delta f_{jk})-B_{rf}}{2\sqrt{2}\sigma}\right\}-erfc\left\{\frac{-2(f_{rf}-\Delta f_{jk})+B_{rf}}{2\sqrt{2}\sigma}\right\}\right].\end{aligned} \tag{3.23}$$

We can obtain the average power of optical signal beat noise falling in bandwidth B_{rf}, $\langle N_{s-s}\rangle$, by ensemble averaging N_{s-s} with the pdf of $\Delta f_{jk}(j,k=1,2,..,M,j\neq k)$.

Finally, the CINR of the regenerated radio signal in the OC connection system is given by

$$CINR_c=\frac{C_0}{N_c+I_0}. \tag{3.24}$$

3.3.2 Optical Switch Connection

In the case of the OSW connection, some optical chip pulses in CDMA signal from k-th RBS may be lost at the OSW of other RBS's which are located between the k-th RBS and the HE, therefore, the chip pulse erasure has to be taken into consideration for the CINR analysis. First, we theoretically derive the average number of 1's in the prime code sequence successfully reaching the HE and next analyze the CINR.

At the OSW of each RBS, an optical IM signal converted from a radio signal is spectrum-spread and simultaneously launched into the fiber-optic bus link. If an IM/CDMA signal from the k-th RBS arrives at the OSW of the j-th ($k>j$) RBS which is transmitting its own signal, a signal collision occurs and causes the erasure of some chip pulses from the k-th RBS. Figure 3.6 illustrates the collision between two IM/CDMA signals. When the collision between two IM/CDMA signals occurs at the OSW of the j-th RBS, we lose IM/CDMA signal from the k-th RBS located farther than the j-th RBS because the multiplexing of IM/CDMA signals is performed by using OSW.

Here, we examine the number of coincidences of 1's between any two prime code sequences in the code word period, T_F. For the 0-th prime code sequence, c_0, the number of coincidences of 1's with any other sequences, $c_n(n\neq 0)$, is always one in the code frame period T_F, and this property is kept for all shifted versions of $c_n(n\neq 0)$. On the other hand, between any other two code sequences, c_m and c_n $(m\neq 0, n\neq 0, m\neq n)$, the number of coincidences of 1's yields none, one, or two. In other words, the peak of the cross-correlation function is 1 between c_0 and $c_n(n\neq 0)$ sequences, and 1 or 2 between c_m and c_n $(m\neq 0, n\neq 0, m\neq n)$. Let N_{mni} the number of the shifted versions of c_m sequences which has i coincidences of 1's with c_n sequences. For a prime number $p=2q-1$, we can find that N_{mni} is

$$N_{0ni}=\begin{cases}0 & ;i=0,2\\ 4q^2-4q+1=p^2 & ;i=1 \text{ for } n=1,2,..,p-1\end{cases}, \tag{3.25}$$

$$N_{mni}=\begin{cases}q^2-q & ;i=0,2\\ 2q^2-2q+1 & ;i=1 \text{ for } m,n=1,2,..,p-1, m\neq n\end{cases}. \tag{3.26}$$

In the code frame period T_F, therefore, the average number of coincidences of 1's is one for any prime code sequence pair. In actual DOS-CDMA CATA system, a code sequence comes into collision with another sequence asynchronously, so we have to consider the partial collision between two chip pulses. For the simplicity of analysis, however, we assume the full chip pulse is lost even in this case.

From above results, when a DOS-CDMA signal from a RBS comes to another OSW, one chip pulse is erased due to the collision on the average. Moreover a DOS-CDMA signal transmitted from the k-th RBS may lost from 1 to (k-1) chip pulses because it passes through (k-1) OSW's to the HE. Hence, letting χ_k denote the average number of chips successfully reaching the HE, χ_k, is given by

$$\chi_k = p-(k-1). \tag{3.27}$$

This is a worst case estimation because the same chip pulse comes into collision with different chip pulses of more than two RBS's. The k-th average received optical power, P_{r_k}, at the output of the SC is given by

$$P_{r_k} = 10\log_{10} P_s + kG' - kL_f - 10\log_{10} M + G_M \text{[dB]} (k=1,2,..,M). \tag{3.28}$$

It is assumed that G_M is equal to $10\log_{10} M$ as the same with the case of OC connection. For easy discussion, we consider $G'=G_c+G_a$ [dB]. G' is the gain of OA at each RBS to compensate the optical loss caused by the chip pulse erasure. We set the value of G_c to keep the carrier power of the radio signal from the farthest M-th RBS equal to that in OC connection at the correlator and G_a[dB] is an additional gain. The gain G_c satisfies the following equation:

$$P_{r_M} \frac{\chi_M}{p^2} = P_s \frac{1}{p}. \tag{3.29}$$

Consequently, the desired G_c is derived as

$$G_c\text{[dB]} = \frac{10}{M}\log_{10}\frac{p}{\chi_M} + L_f \tag{3.30}$$

and the average received optical power, P_{r_k}, at the k-th correlator is given by

$$P_{r_k} = P_s\left(\frac{p}{\chi_M}\right)^{k/M} g_a{}^k, \tag{3.31}$$

where $G_a = 10\log_{10} g_a$.

The carrier power of the k-th radio signal regenerated at HE can be written as

$$C_k=C_0\left(\frac{\chi_k}{p}\right)^2\left(\frac{p}{\chi_M}\right)^{2k/M} g_a{}^{2k}(k=1,2,..,M). \tag{3.32}$$

On the other hand, IM/CDMA signals from RBS's located farther than the k-th RBS never reach at the k-th correlator because they are erased at the OSW of the k-th RBS during the interval of 1's in $c_k(t)$ as shown in Fig.3.6. Thus, we consider only the IM signals from RBS's nearer than the k-th RBS as the interference, then the interference power contaminating the k-th radio signal regenerated at HE can be written as

$$I_k=\frac{\sigma_c^2}{p^2}\sum_{j=1}^{k-1}C_j. \tag{3.33}$$

Hence, the CIR of k-th radio signal in the OSW connection system is given by

$$CIR_k=\frac{C_k}{I_k}=\varepsilon_k CIR_0(k=1,2,..,M), \tag{3.34}$$

$$\varepsilon_k=\frac{M-1}{\sum_{j=1}^{k-1}\left(\frac{p}{\chi_M}\right)^{2(j-k)/M}\left(\frac{\chi_j}{\chi_k}\right)^2 g_a{}^{2(j-k)}}, \tag{3.35}$$

where CIR_0 is the CIR obtained in the OC connection system(Eq.(3.8)).

In the OSW connection system, since IM/CDMA signals from RBS's located farther than the k-th RBS never reach the k-th correlator, relative intensity noise, shot noise, beat noise among ASE of an OA and optical signal and beat noise among ASE's are different from those in the OC connection system as in the followings:

$$N'_{RIN}=\zeta_{RIN}\left(\frac{\alpha P_{r_k}}{p^2}\right)^2(\chi_k^2+k-1)B_{rf}(k=1,2,..,M), \tag{3.36}$$

$$N'_{shot}=2e\left[\frac{\alpha P_{r_k}}{p^2}(\chi_k+k-1)+\alpha\left\{N'_{sp}\sum_{j=1}^{k}\left(\frac{g'}{l_f}\right)^j+MN_{spM}\right\}W\right]B_{rf}(k=1,2,..,M), \tag{3.37}$$

$$N'_{s-sp}=4\alpha\left\{N'_{sp}\sum_{j=1}^{k}\left(\frac{g'}{l_f}\right)^j+MN_{spM}\right\}\frac{\alpha P_{r_k}}{p^2}(\chi_k+k-1)B_{rf}(k=1,2,..,M), \tag{3.38}$$

$$N'_{sp-sp}=2\alpha^2\left\{N'_{sp}\sum_{j=1}^{k}\left(\frac{g'}{l_f}\right)^j+MN_{spM}\right\}^2\left(W-f_{rf}\right)(k=1,2,..,M), \tag{3.39}$$

where $G'=10\log_{10}g'$, $L_f=10\log_{10}l_f$ [dB] and N'_{sp} is given by Eq.(3.17) substituted $G=G'$. Note that in OSW connection, no optical signal beat noise occurs that is different from the OC connection. Therefore, the total noise power at the k-th correlator output, N_{swk}, is

$$N_{swk}=N'_{RIN}+N'_{shot}+N_{th}+N'_{s-sp}+N'_{sp-sp}(k=1,2,..,M), \tag{3.40}$$

and the CINR of the k-th regenerated radio signal, $CINR_k$, is given by

$$CINR_k=\frac{C_k}{I_k+N_{swk}}(k=1,2,..,M). \tag{3.41}$$

3.4 Numerical Results and Discussions

In this section, some numerical results of CINR in the DOS-CDMA CATA system for both the OC and the OSW connections are shown and discussed. Parameters used for calculation are shown in Table 3.3.

Figure 3.7 shows the CIR of the k-th RBS for the prime number, p=23 and the number of connected RBS's, M=20. In the case of G_a=0dB, the CIR in the OSW connection system is degraded compared with the OC connection system as k comes near to M because the coefficient ε_k(Eq.(3.35)) which expresses the CIR reduction effect due to the erasure of chip pulse becomes less than 1 as k comes near to M. On the other hand, the CIR of the nearer RBS to the HE in the OSW connection system is more improved compared with the OC connection system because IM/CDMA signals from RBS's located farther than the k-th RBS never reach the k-th correlator, therefore the interference power is reduced. However, Eqs.(3.34) and (3.35) show that by increasing the additional gain, G_a, the CIR_k can be improved for any k-th radio signal. Figure 3.7 shows that as the G_a increases, the CIR_k is improved and we can obtain almost the same CIR for all radio signals from M RBS's. On the other hand, the additional gain is not effective to improve the CIR in the OC connection system because the radio signals from the nearer RBS to the HE suffer interferences with amplified large power while the CIR of the

Table 3.3 Parameters used for calculation.

Responsivity of PD	α	0.8A/W
PSD of the relative intensity noise	ζ_{RIN}	-152dB/Hz
Bandwidth of optical filter	W	1THz
Noise temperature	T	300K
Load resistance	R_L	50 Ω
Spontaneous emission factor of OA	η_{sp}	2.0
Quantum efficiency of the OA	η_a	0.5
Radio signal frequency	f_{rf}	1.93GHz
Radio signal bandwidth	B_{rf}	900KHz
Coupling plus insertion loss of OC	L_{oc}	3dB
Fiber loss between RBS's	L_f	0.5dB
FWHM of the LD	$\Delta\nu_{LD}$	10MHz
Difference of center frequency of the LD	Δ_F	1THz

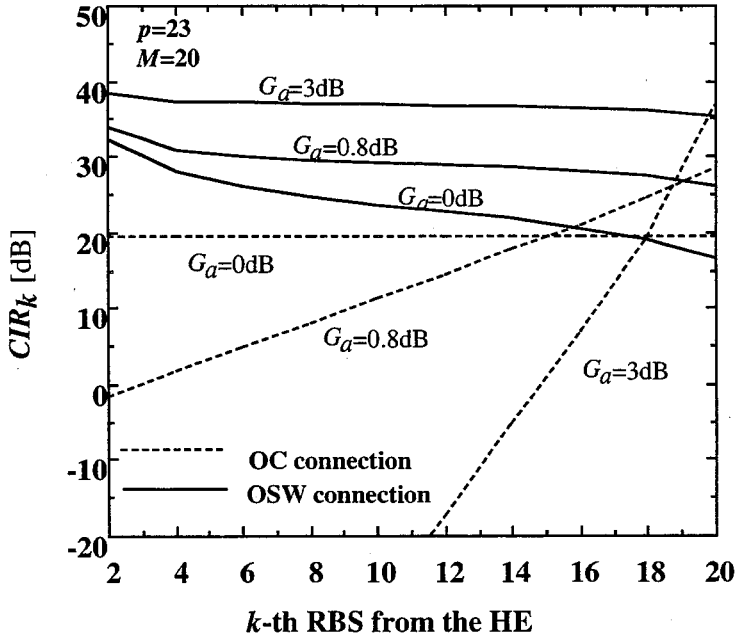

Fig.3.7 CIR of the k-th RBS from the HE for p=23 and M=20.

radio signal from the farther RBS can be improved as shown in Fig.3.7.

Figure 3.8 shows the CIR of the farthest M-th RBS as a function of prime code number, p for M of 20, 40 and 80. The upper abscissa is the switching speed of OSW. When G_a is 0dB in the OSW connection system, the coefficient ε_M is less than 1 as p comes near to M, thus the CIR_M of the farthest M-th RBS is degraded compared with the OC connection system. This is due to the erasure of chip pulse of the M-th radio signal. However, this penalty can be reduced and the CIR_M comes to the same as that in the OC connection system as p increases more than M. It is also found from Fig.3.8 that by introducing additional gain(G_a>0dB), the CIR_M of the farthest M-th RBS is more improved than that in the OC connection system as G_a increases for any p and M. This is because as p increases more than M, Eq.(3.35) shows that ε_M comes near to $\frac{M-1}{\sum_{j=1}^{M-1} g_a^{2(j-M)}}$ which is more than 1 and yields the same value regardless of M.

Here, we have to consider the limitations in G_a and p to realize the OSW connection system. Regarding p, the achievable switching speed of the OSW gives the limitations of the prime code number, p. If we use the OSW with its speed of almost 10GHz for the case of B_{rf}=900KHz, we can increase the p up to about 80.

The possible additional gain, G_a, is limited by the optical power limitation in the optical fiber. Figure 3.9 shows the relationship between the average received optical power from the farthest M-th RBS, P_{r_M} normalized by the average transmitted optical power, P_{r_M}/P_s, and the number of connected RBS's, M in the case of p=79 ($1/T_c$=11.2GHz). For example, in the case that the limitation of $\frac{P_{r_M}}{P_s}$ is 20dB, the upper limits in numbers of connected RBS's in OSW connection system are 63, 41, 30, 23 and 19 for G_a= 0.2, 0.4, 0.6 , 0.8 and 1dB's respectively. G_a can be increased up to 0.8dB for $\frac{P_{r_M}}{P_s}$ = 20dB and M=20. Thus it is seen from Fig.3.8 that for M=20, the CIR in the OSW connection system can be more improved by about 8dB than that in the OC connection system by introducing the G_a of 0.8dB.

Figure 3.10 shows the CNR as a function of prime code number p for P_S of 0dBm and M

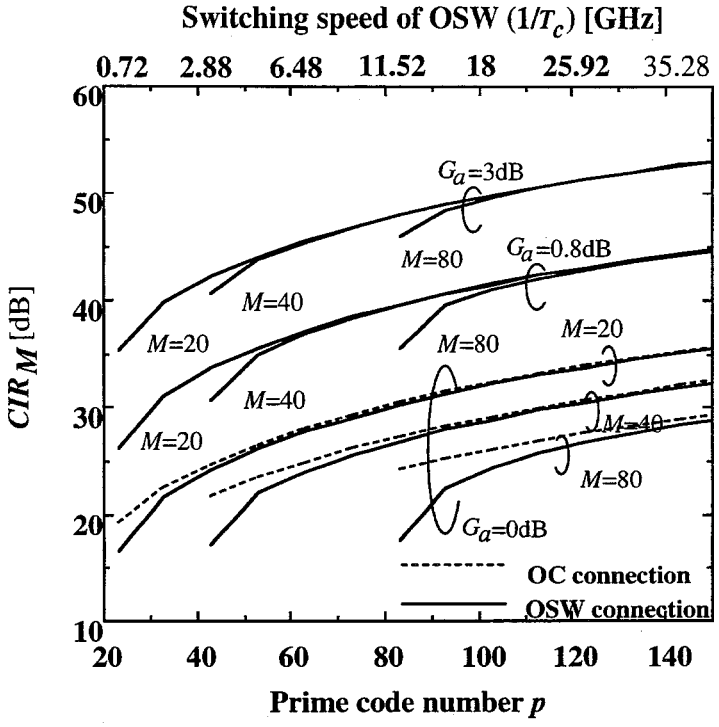

Fig. 3.8 CIR of the farthest M-th RBS versus prime code number, p for M of 20, 40 and 80.

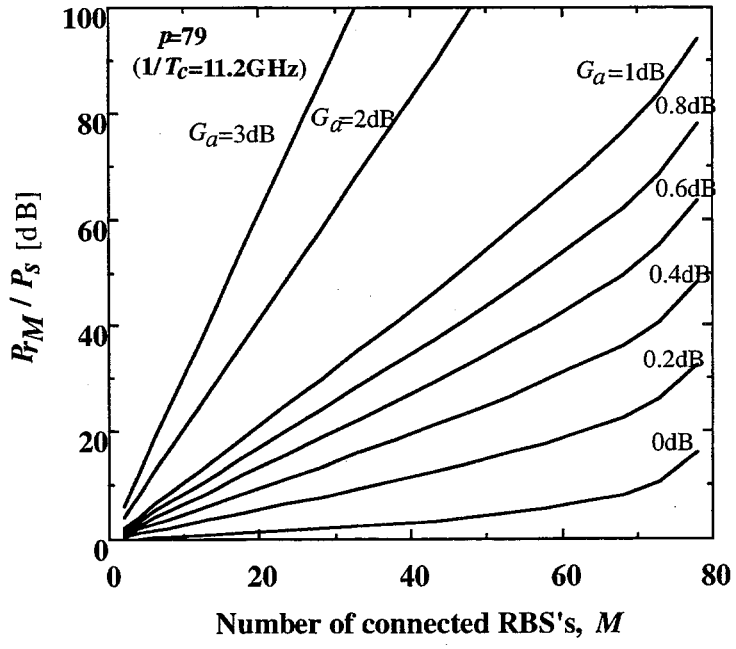

Fig.3.9 Relationship between P_{r_M} / P_s and M for p=79 in the OSW connection system.

of 20 and 40. When G_a is 0dB, CNR's for both OC and OSW connection systems are dominated by the beat noise among ASE of an OA and the optical signal, N_{s-sp} and N'_{s-sp}, respectively for small p but affected by the receiver thermal noise, N_{th} , as p comes to large because the carrier power decreases in proportion to $\frac{1}{p^2}$. As p comes near to M, the CNR in the OSW connection system is degraded by the erasure of chip pulse compared with the OC connection system. However, the CNR's of both OC and OSW connection systems are similar as p increases more than M because the erasure of chip pulse can be neglected and N_{s-sp} and N'_{s-sp} are dominated by the OA at the output of SC. On the other hand, when G_a is more than 0dB, the CNR in the OSW connection system is dominated by N'_{s-sp} caused by the OA at the RBS, thus, the CNR is more improved than that in the OC connection system as G_a increases. For example, it is seen from Fig.3.10 that for P_S =0dBm, M=20 and p=79, the CNR in the OSW connection system with G_a of 0.8dB can be more improved by 11dB than that in the OC connection system.

It is seen from Figs.3.8 and 3.10 that the CINR is dominated by the CIR for any p. By introducing additional gain, the CINR in the OSW connection system can be more improved than that in the OC connection system. It is found that for M=20, the CINR in the OSW connection system can be more improved by about 8dB than that in the OC connection system by introducing the G_a of 0.8dB.

Figure 3.11 shows the CINR as a function of the number of connected RBS's, M, for p=79 ($1/T_c$=11.2GHz) and P_S=0dBm. In the OSW connection system, when G_a=0dB and M comes near to p, the CIR is worse than the OC connection system. However, the CINR of the OSW connection system is more improved than that in the OC connection system as G_a increases. In the OC connection system, the number of connected RBS's is determined by the required CINR. On the other hand, in the OSW connection system, the number of connected RBS's is determined by both the required CINR and the optical power limitation. It is seen from Figs.3.9 and 3.11 that when the required CINR is 30dB and the required $\frac{P_{rM}}{P_S}$ is 20dB, the numbers of connected RBS's in the OSW connection system are 63, 41, 30 and 23 for G_a= 0.2, 0.4, 0.6 and 0.8dB's respectively, while the number of connected RBS's in the OC connection system is 18.

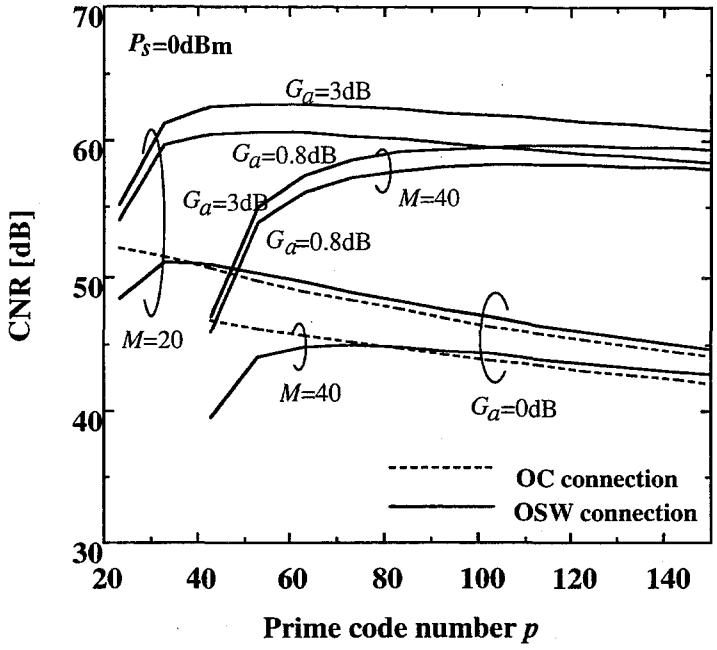

Fig. 3.10 CNR versus prime code number, p for P_S=0dBm and M of 20 and 40.

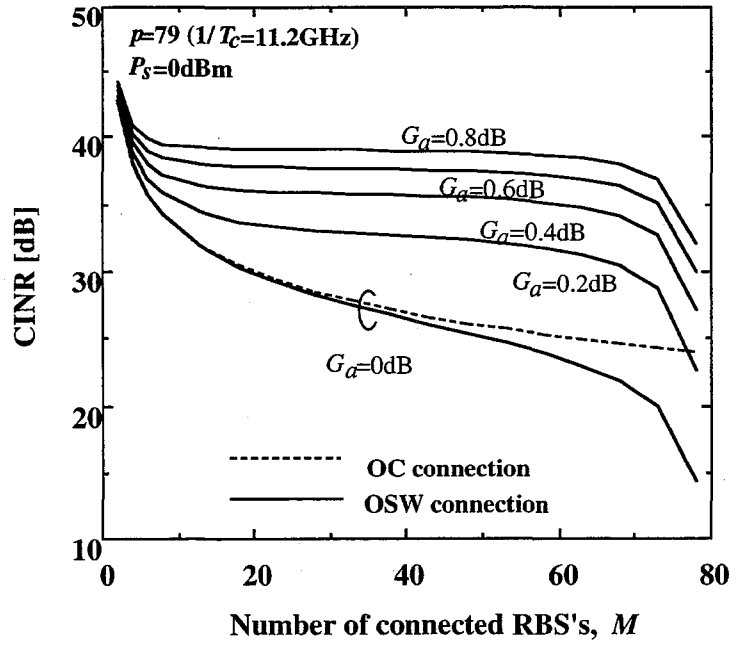

Fig. 3.11 CINR versus number of connected RBS's, M for p=79 ($1/T_c$=11.2GHz).

Thus it is found that in the OSW connection system with G_a=0.2dB, three times of RBS's can be connected to the CATA system compared with the OC connection system.

3.5 Concluding Remarks

In this chapter, we have investigated the direct optical switching(DOS) CDMA method for fiber-optic radio networks including CATA systems where the concept of FTTA is applied to CATV systems. The configuration of the DOS-CDMA CATA system has been proposed by using optical coupler and optical switch connections. We have theoretically analyzed the carrier to interference-plus-noise ratios of regenerated radio signals at the head end for two types of bus connection methods considering the chip pulse erasure at the optical switch. Following results are obtained:

1. In the optical switch connection system, by introducing the additional optical gain at each radio base station, the carrier to interference power ratios for all radio base stations can be almost the same as those in the prime code number increases more than the number of connected radio base stations.
2. In the optical switch connection system with the additional gain, the carrier to interference-plus-noise power ratio (CINR)s for all radio base stations and the number of connected radio base stations can be improved compared with the optical coupler connection system. For example, by using the optical switch connection system with additional gain, G_a=0.2dB, three times of radio base stations can be connected to the CATA system with the CINR of 30dB and the average received optical power from the farthest RBS normalized by the average transmitted optical power of 20dB for prime number, p=79, compared with the optical coupler connection system.

Thus the optical switch connection is an effective DOS-CDMA CATA system where an optical switch is used not only to spread the spectrum of optical signals but also to launch them into the fiber-optic bus link.

Chapter 4
Optical Polarity Reversing Correlator (OPRC) for DOS-CDMA Using PN codes

4.1 Introduction

In the direct optical switching (DOS)-CDMA method described in the Chapter 3, only optical uniphase orthogonal codes such as prime codes [16]-[19] are applied to obtain a desired process gain because an optical switch is used to correlate DOS-CDMA signals at each correlator. However, the prime code suffers a limit in the number of distinct code sequences, which results in the limitation of the number of radio base stations connected to fiber-optic radio networks. Besides in fiber-optic radio networks using the DOS-CDMA scheme with prime codes, the optical power efficiency is low because the pulse duty of a prime code is quite low. Therefore, we should consider a new type of the correlator for the DOS-CDMA method to which PN codes such as Maximal length codes and Gold codes can be applied because those codes are usually used in radio systems and generally superior in the number of distinct code sequences compared with prime codes. For digital networks using the optical CDMA method, the sequence inversion keyed(SIK) direct sequence(DS) CDMA methods that have been proposed in Refs.[31]-[32], require specially balanced PN codes. In order to allow the use of any unbalanced PN codes, the power splitting ratio of the power divider at the optical correlator has been controlled [33], and the transmission of two channels using two wavelengths or two orthogonal polarizations has been proposed [34]. In SIK-CDMA methods, however, binary digital data are encoded and transmitted with the positive polarity and the negative polarity of bipolar codes, thereby their

correlators at the receiver can not be applied to DOS-CDMA signals that are converted from radio signals by the on-off switching CDMA method. In this thesis, we newly propose the optical polarity reversing correlator(OPRC) for the DOS-CDMA radio highway network using PN codes [35]-[39].

4.2 Direct Optical Switching(DOS) CDMA Radio Networks Using OPRC

4.2.1 Principle of OPRC

The optical polarity-reversing correlator(OPRC) can be realized with various optical devices such as optical switch(OSW)es, matched filters and Mach-Zehnder Interferometer(MZI)s. We realize the OPRC with a MZI or two OSW's. Figure 4.1 illustrates the configuration of the transmitter and the OPRC for the optical CDMA using the PN code $c_k(t)$ having the value of 1 or -1. The $c_k(t)$ has the frame period, T_F, and the chip width, T_c. In the interval of T_F, $c_k(t)$ has the code length L which is the number of chips and the number of 1's of $\frac{L+1}{2}$. At the k-th RBS, LD is directly modulated by the radio signal with the optical modulation index of 1. DOS-CDMA is performed at OSW driven with the biased PN code $\frac{1+c_k(t)}{2}$. Then, the intensity of optical signal from the k-th RBS is written by

$$I_k(t)=P_s\{1+g_k(t)\}\frac{1+c_k(t)}{2}, \tag{4.1}$$

where $g_k(t)$ is the radio signal with the bandwidth B_{rf} and the carrier frequency f_{rf} and P_s is the average transmitted optical power before the optical switching.

At the k-th OPRC, many IM/CDMA signals are received and split into two signals at the MZI or the optical coupler(OC). It is assumed that the biased PN code, $\frac{1+c_k(t)}{2}$, matched with the one at the RBS is regenerated at the CS by using the retiming code generator such as the retiming block [44] and the synchronization between two code sequences is taken. The OPRC is

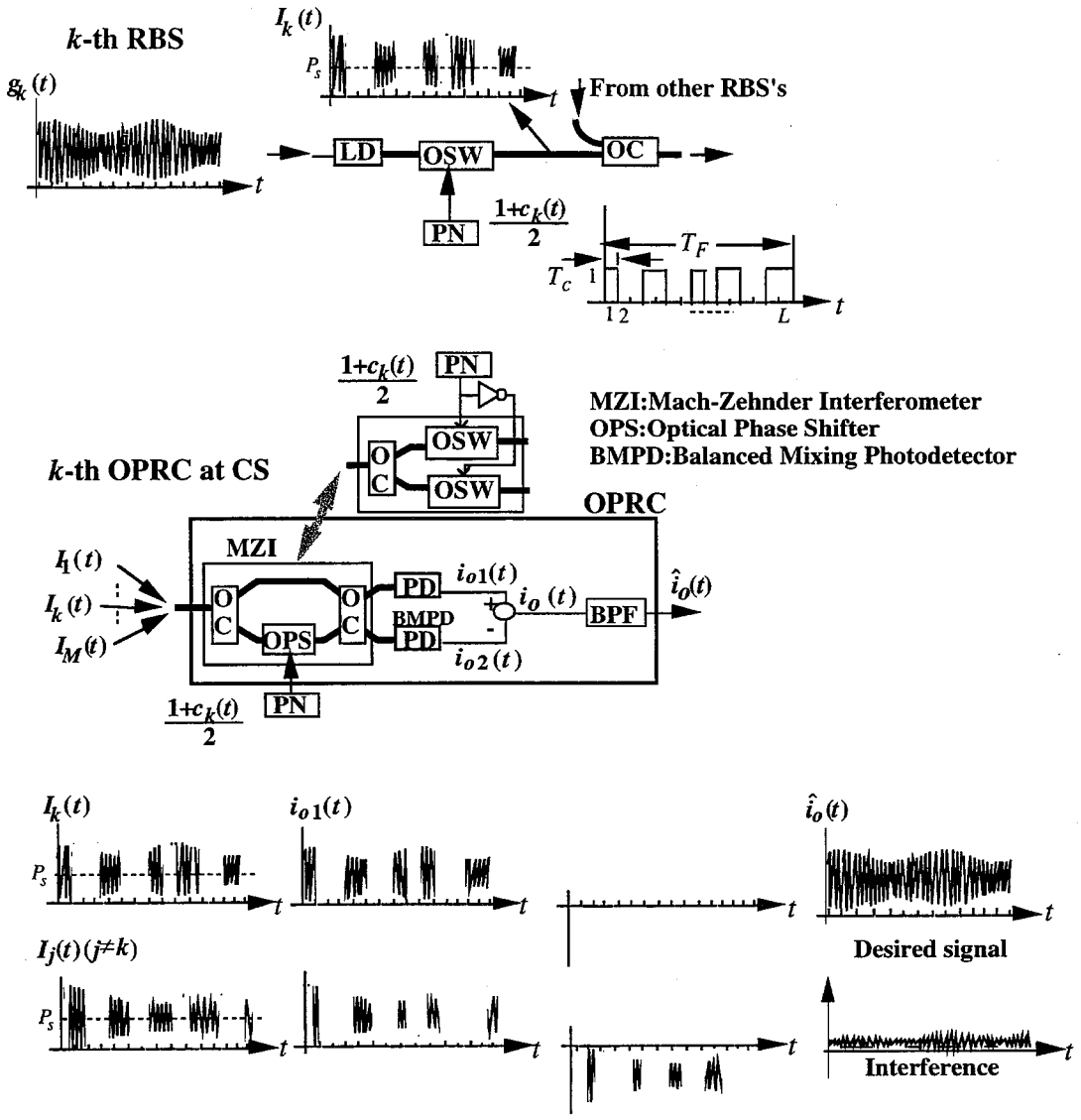

Fig.4.1 Configuration of the transmitter and the OPRC for optical CDMA using PN codes.

driven by the biased PN code, $\frac{1+c_k(t)}{2}$, matched with the one at the RBS. In the case of the OPRC realized with a MZI, the phase of the OPS(optical phase shifter) is shifted according to the biased PN code, $\frac{1+c_k(t)}{2}$. When $\frac{1+c_k(t)}{2}$ is 1, the phase difference between both arms of MZI is zero, thus IM/CDMA signals are outputted to the upper port of MZI through the second OC. When $\frac{1+c_k(t)}{2}$ is 0, the phase difference between both arms of MZI is set to π, thus the lower port of MZI outputs IM/CDMA signals through the second OC. In the case of OPRC realized with two OSW's, when $\frac{1+c_k(t)}{2}$ is 1 the upper OSW is set to on and the lower OSW is set to on when $\frac{1+c_k(t)}{2}$ is 0.

Thus output currents of the BMPD(balanced mixing photodetector) are expressed as

$$i_{o1}(t)=\alpha \sum_{j=1}^{M} P_{r_k} g_j(t)\frac{1+c_j(t)}{2}.\frac{1+c_k(t)}{2}+i_{n1}(t), \tag{4.2}$$

$$i_{o2}(t)=\alpha \sum_{j=1}^{M} P_{r_k} g_j(t)\frac{1+c_j(t)}{2}.\frac{1-c_k(t)}{2}+i_{n2}(t), \tag{4.3}$$

where α is the responsivity of the PD, and $i_{n1}(t)$ and $i_{n2}(t)$ are additive noise currents, respectively. Eqs.(4.2) and (4.3) show that the positive polarity of the desired k-th code $c_k(t)$ matches with the k-th one at the RBS at the upper port of MZI or the upper OSW, on the other hand it is obstructed at the lower port of MZI or the lower OSW. The desired k-th signal at the input to the BPF is a bandpass natural sampled signal converted from the k-th radio signal, $g_k(t)$, because an optical switching is a window-type sampling. Therefore, a radio signal is conveyed by the optical carrier with its signaling format kept and can be regenerated from the pulsed signals by the interpolation at the BPF [29][43] whose principle will be discussed in Sect.4.3.

On the other hand, for the interference signal $I_j(t)(j\neq k)$, both ports of MZI or both OSW's generate interferences only when the positive polarity of $c_j(t)$ coincides with the positive or negative polarity of $c_k(t)$. Two interferences of BMPD are subtracted and the interference is suppressed at the BPF. However, in the unipolar type correlator for optical CDMA, PN codes can not be applied because the interference is not suppressed though the code sequence length increases. The detail will be discussed in Sect.4.3.

4.2.2 System Configuration

Figure 4.2 illustrates the configuration of the optical CDMA radio highway network using the OPRC.

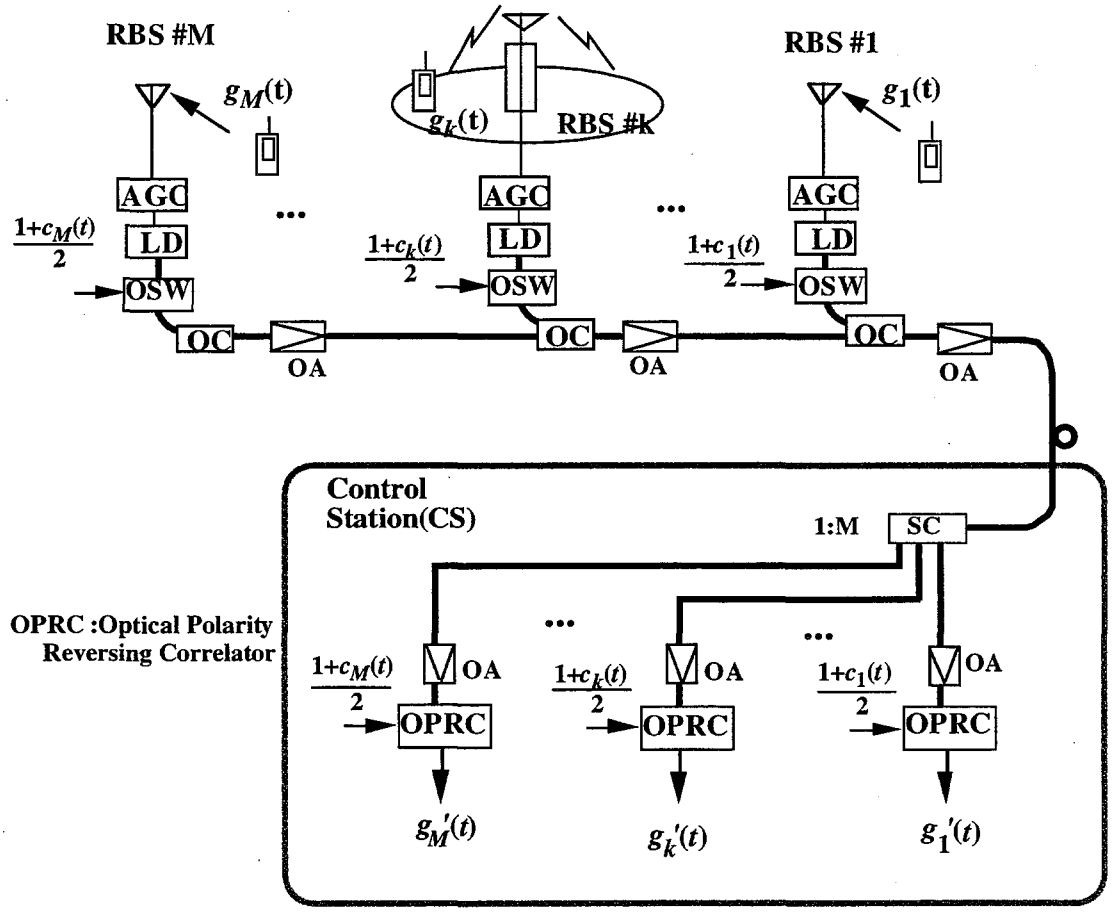

Fig.4.2 Configuration of the optical CDMA radio highway network using the OPRC.

Each RBS is equipped with an automatic gain controller (AGC) to control the amplitude of a received radio signal in order to keep the optical modulation index constant at the LD. After the direct intensity-modulation(IM) at the LD, the direct optical switching(DOS) CDMA is performed by on-off switching at the OSW driven by a biased PN code. In the bus link, many IM/CDMA signals from M RBS's are multiplexed by the DOS-CDMA method and transmitted to the CS. When any biased PN code sequence coincides with another biased PN code sequence, the numbers of coincidences of chips is $\frac{(L+1)^2}{4L}$ out of chips of L. In the case of the fiber-optic bus link using the OSW connection, the signal collision at the OSW of each RBS will cause the erasure of enormous chip pulses in DOS-CDMA signals. As the enough additional gain can not be inserted at each RBS owing to the optical power limitation, the far-near problem will happen in the fiber-optic link. Thus we consider a system configuration using only the OC connection.

At the CS, optical CDMA signals are at first power-split to each of M receivers. IM/CDMA signals are correlated at the OPRC driven by a biased PN code matched with the RBS. To compensate the optical loss between RBS and the receiver, each RBS and CS are equipped with OA's. At the k-th OPRC, the average received optical power, P_{rk}, can be written as

$$P_{rk}=10\log_{10} P_s-k(L_f+L_{oc})+kG-10\log_{10} M+G_M-2L_{oc}[\text{dB}], \tag{4.4}$$

where L_{oc}[dB] , L_f[dB], G[dB] and G_M[dB] are the coupling loss plus the insertion loss of an OC, the fiber loss between RBS's, the gain of OA at the RBS and the gain of OA at the output of 1:M SC, respectively. The last term $2L_{oc}$ is the coupling loss caused by the two OC's at the MZI in the Fig.4.1.

4.3 Theoretical Analysis of Carrier-to-Interference-plus-Noise Ratio Performance

The input current to the BPF is given by

$$\begin{aligned} i_o(t)&=i_{o1}(t)-i_{o2}(t) \\ &=i_{S_k}(t)+i_I(t)+i_N(t), \end{aligned} \tag{4.5}$$

where $i_{S_k}(t)$, $i_I(t)$ and $i_N(t)$ are the desired signal, the interference and the additive noise, respectively. In order to have the same optical received power at the OPRC, we assume that an OA equipped at each RBS has the gain G of L_f+L_{oc} and the gain of OA at the output of SC, G_M, is equal to $10\log_{10} M+2L_{oc}$. Thus, the same received power $P_{r_k}=P_s$ $(k=1,2,..,M)$ is obtained from Eq.(4.4). It is also assumed that each MZI receives M optical signals with the same modulation index of 1. At the input of the BPF, $i_{S_k}(t)$ and $i_I(t)$ are expressed as

$$i_{S_k}(t)=\alpha P_s g_k(t)\frac{1+c_k(t)}{2}, \tag{4.6}$$

$$i_I(t)=\sum_{j=1,j\neq k}^{M}\alpha P_s g_j(t)\frac{1+c_j(t)}{2}c_k(t), \tag{4.7}$$

respectively.

We consider the carrier power of regenerated radio signal and the interference power at the BPF from the power spectral density(PSD)s of the desired signal and the interference. The autocorrelation of desired signal, $i_{S_k}(t)$, is expressed as

$$R_S(\tau)=(\frac{\alpha P_s}{2})^2 R_g(\tau)\{1+\frac{2}{L}+R_c(\tau)\}, \tag{4.8}$$

where $R_g(\tau)$ and $R_c(\tau)$ are the autocorrelations of $g_k(t)$ and $c_k(t)$, respectively. Though we assume that radio signals, $g_j(t)$ $(j=1,2,..,M)$, are unmodulated carriers, the calculated carrier power of regenerated radio signals can be applied irrespective of the modulation method of radio signals. Thus we assume that radio signals, $g_j(t)$ $(j=1,2,..,M)$, are unmodulated carriers which have the autocorrelation function, $R_g(\tau)$,

$$R_g(\tau)=\frac{1}{2}\cos(2\pi f_{rf}\tau). \tag{4.9}$$

The autocorrelations of $c_k(t)$ is given by [48]

$$R_c(\tau)=\frac{1}{L^2}+\frac{L+1}{L^2}\sum_{k=-\infty,k\neq 0}^{\infty}\mathrm{sinc}^2(\frac{\pi k T_c}{T_F})\cos(\frac{2\pi k\tau}{T_F}). \tag{4.10}$$

Thus, the PSD of $i_{S_k}(t)$, $S_S(f)$, is given by

$$S_S(f)=(\frac{\alpha P_s}{2})^2\left\{S_g(f)(1+\frac{2}{L})+S_g(f)\otimes S_c(f)\right\}$$
$$=(\frac{\alpha P_s}{2})^2\left\{(\frac{L+1}{L})^2 S_g(f)+\frac{L+1}{L^2}\sum_{k=-\infty,k\neq 0}^{\infty}\mathrm{sinc}^2(\frac{\pi k T_c}{T_F})S_g(f-k/T_F)\right\}, \quad (4.11)$$

where $S_g(f)$ and $S_c(f)$ are the PSD's of $g_k(t)$ and $c_k(t)$, respectively. The first term of $S_S(f)$ is the desired signal component around f_{rf} and - f_{rf}, and the second terms are the frequency shifted components caused by bandpass sampling. Images of these shifted components will cause the distortion in the desired signal as the self-interference if they overlap over the signal. However, we can perfectly remove the self-interference components by setting the value of the radio frequency f_{rf} at $(j+1/2)B_{rf}$ or j/T_c (j is an integer). Without such special values of f_{rf}, we can ignore the self-interference component because it may not deteriorate the signal quality [29]. Since the biased PN code sequence drives the OSW periodically with the sampling period T_F at the RBS transmitter, each signal pulse in one code sequence period has the same period T_F. Then, if the periodic frequency $1/T_F$ is set to be at least twice radio signal bandwidth(=2 B_{rf}), the radio signal can be regenerated from only one pulse train in the code sequence by the interpolation at the BPF [43].

From Eq.(4.11), C can be obtained as

$$C=\frac{1}{2}(\frac{\alpha P_s(L+1)}{2L})^2. \quad (4.12)$$

The autocorrelation of $i_I(t)$, $R_I(\tau)$, is derived as

$$R_I(\tau)=(M-1)(\frac{\alpha P_s}{2})^2 R_g(\tau)\{R_c(\tau)(1+\frac{2}{L})+R_\gamma(\tau)\}, \quad (4.13)$$

where $R_\gamma(\tau)$ represents the autocorrelation of $c_i(t).c_k(t)$. $R_\gamma(\tau)$ is given by [49]

$$R_\gamma(\tau)=\overline{a_0^2}+\sum_{k=-\infty,k\neq 0}^{\infty}\frac{1}{L}\frac{1}{1+(k\pi/L)}\cos(\frac{2\pi k\tau}{T_F}), \quad (4.14)$$

where the value of $\overline{a_0^2}$ depends on the kind of used code sequence. The Maximal length code is usually used in radio system and Refs. [16],[47] and [49] have reported that the Gold code is a excellent code as a PN code which can provide the small cross-correlation. Thus Gold codes and Maximal length codes are used for the optical CDMA using the OPRC. $\overline{a_0^2}$'s for Gold codes and Maximal length codes are given by [47]-[49]

$$\overline{a_0^2}=\begin{cases}\dfrac{L^2+L-1}{4L^3} & \text{for Gold codes}\\ \dfrac{L^2+L-1}{L^3} & \text{for Maximal length codes}\end{cases}. \tag{4.15}$$

The PSD of $i_I(t)$, $S_I(f)$, is given by

$$\begin{aligned}S_I(f)&=(M-1)(\frac{\alpha P_s}{2})^2 S_g(f)\otimes\{S_c(f)(1+\frac{2}{L})+S_\gamma(f)\}\\ &=(M-1)(\frac{\alpha P_s}{2})^2[(\frac{L+2}{L^3}+\overline{a_0^2})S_g(f)\\ &+\sum_{k=-\infty,k\neq 0}^{\infty}\{\frac{(L+1)(L+2)}{L^3}\mathrm{sinc}^2(\frac{\pi kT_c}{T_F})+\frac{1}{L}\frac{1}{1+(k\pi/L)}\}S_g(f-\frac{k}{T_F})]\end{aligned}, \tag{4.16}$$

where $S_\gamma(f)$ is the PSD of $c_i(t).c_k(t)$. The interference power at the output of the BPF, I, can be obtained as

$$I=\begin{cases}\dfrac{M-1}{2}(\dfrac{\alpha P_s}{2})^2\dfrac{L^2+5L+7}{4L^3} & \text{for Gold codes}\\ \dfrac{M-1}{2}(\dfrac{\alpha P_s}{2})^2\dfrac{(L+1)^2}{L^3} & \text{for Maximal length codes}\end{cases}. \tag{4.17}$$

Hence, from Eqs.(4.12) and (4.17) the CIR(carrier-to-interference power ratio)s for Gold codes and Maximal length codes are written by

$$CIR=\begin{cases}\dfrac{4}{M-1}\dfrac{L(L+1)^2}{L^2+5L+7} & \text{for Gold codes}\\ \dfrac{L}{M-1} & \text{for Maximal length codes}\end{cases}. \tag{4.18}$$

For discussion, we consider the CIR in the case of unipolar type correlator for optical CDMA as shown in Fig.3.2. When prime codes are applied, the CIR is given by [29][30]

$$CIR_{uc,p}=\frac{1}{(M-1)}\frac{p^2}{\sigma_c^2}\ \text{for prime codes}, \tag{4.19}$$

where σ_c^2 denote the average variance of the cross-correlation of the prime code, whose length, L, is p^2. On the other hand, when PN codes are applied to the unipolar type correlator as the same with the proposed OPRC, from Eq.(4.2), the interference current at the input of BPF is

given by

$$i_{I,uc}(t)=\sum_{j=1,j\neq k}^{M}\frac{\alpha P_s}{4}g_j(t)\{1+c_j(t)\}\{(1+c_k(t)\}. \tag{4.20}$$

Autocorrelation function of $i_{I,uc}(t)$, $R_{I,uc}(\tau)$, is given by

$$R_{I,uc}(\tau)=(M-1)(\frac{\alpha P_s}{4})^2 R_g(\tau)\{1+\frac{4}{L}+\frac{4}{L^2}+2(1+\frac{2}{L})R_c(\tau)+R_\gamma(\tau)\}. \tag{4.21}$$

The PSD of $i_{I,uc}(t)$, $S_{I,uc}(f)$, is given by

$$\begin{aligned}S_{I,uc}(f)&=(M-1)(\frac{\alpha P_s}{4})^2[S_g(f)(1+\frac{4}{L}+\frac{4}{L^2})+S_g(f)\otimes\{2(1+\frac{2}{L})S_c(f)+S_\gamma(f)\}]\\&=(M-1)(\frac{\alpha P_s}{4})^2[\{1+\frac{4}{L}+\frac{4}{L^2}+\frac{2(L+2)}{L^3}+\overline{a_0^2}\}S_g(f)\\&+\sum_{k=-\infty,k\neq 0}^{\infty}\{\frac{2(L+1)(L+2)}{L^3}\mathrm{sinc}^2(\frac{\pi kT_c}{T_F})+\frac{1}{L}\frac{1}{1+(k\pi/L)}\}S_g(f-\frac{k}{T_F})]\end{aligned}. \tag{4.22}$$

The interference power at the output of the BPF can be obtained as

$$I_{uc}=\begin{cases}\frac{M-1}{2}(\frac{\alpha P_s}{4})^2(1+\frac{17L^2+25L+18}{4L^3}) & \text{for Gold codes}\\ \frac{M-1}{2}(\frac{\alpha P_s}{4})^2(1+\frac{5L^2+7L+3}{L^3}) & \text{for Maximal length codes}\end{cases}. \tag{4.23}$$

Hence, in the case of unipolar type correlator using PN codes, the CIR is written by

$$CIR_{uc}=\begin{cases}\frac{4}{M-1}\frac{4L(L+1)^2}{4L^3+17L^2+25L+15} & \text{for Gold codes}\\ \frac{4}{M-1}\frac{L(L+1)^2}{L^3+5L^2+7L+3} & \text{for Maximal length codes}\end{cases}. \tag{4.24}$$

We analyze the noise power at the output of BPF. We consider additive noise currents composed of the relative intensity noise, the shot noise, the receiver thermal noise, the beat noise between optical signal and amplified spontaneous emission(ASE), the beat noise between ASE's and optical signal beat noise. The total noise power, N, is written by

$$N=N_{RIN}+N_{shot}+N_{th}+N_{s-sp}+N_{sp-sp}+\langle N_{s-s}\rangle, \tag{4.25}$$

When any biased PN code sequence coincides with the positive and the negative polarity of any

PN code sequence, the numbers of coincidences of 1's in the interval of T_F are $\frac{(L+1)^2}{4L}$ and $\frac{L^2-1}{4L}$ respectively. Each noise power is given by

$$N_{RIN}=\zeta_{RIN}\left(\frac{\alpha P_s}{L}\right)^2\left[\left(\frac{L+1}{2}\right)^2+(M-1)\left\{\left(\frac{(L+1)^2}{4L}\right)^2+\left(\frac{L^2-1}{4L}\right)^2\right\}\right]B_{rf}, \tag{4.26}$$

$$N_{shot}=2e\left\{\left(\frac{\alpha P_s}{L}\right)\frac{M(L+1)}{2}+\alpha M(N_{sp}+N_{sp_M})W\right\}B_{rf}, \tag{4.27}$$

$$N_{th}=\frac{8k_BT}{R_L}B_{rf}, \tag{4.28}$$

$$N_{s-sp}=4\alpha M(N_{sp}+N_{sp_M})\left(\frac{\alpha P_s}{L}\right)\frac{M(L+1)}{2}B_{rf}, \tag{4.29}$$

$$N_{sp-sp}=2\alpha^2M^2\left(N_{sp}+N_{sp_M}\right)^2\left(W-f_{rf}\right), \tag{4.30}$$

where e, ζ_{RIN}, W, k_B, T and R_L are the electric charge, the PSD of the relative intensity noise, the bandwidth of optical filter at the CS, Boltzmann constant, the noise temperature and the load resistance, respectively. The PSD's of the ASE, N_{sp} and N_{sp_M}, are given by

$$N_{sp}=\frac{\eta_{sp}}{\eta_a}\cdot\frac{10^{G/10}-1}{10^{G/10}}h\nu, \tag{4.31}$$

$$N_{sp_M}=\frac{\eta_{sp}}{\eta_a}\cdot\frac{10^{G_M/10}-1}{10^{G_M/10}}h\nu, \tag{4.32}$$

respectively, where η_{sp}, η_a and $h\nu$ are the spontaneous emission factor, the quantum efficiency of the OA and the photon energy, respectively [6]. The optical signal beat noise, $\langle N_{s-s}\rangle$, is due to an interference between two optical signals. $\langle N_{s-s}\rangle$ is composed of two interference components: one is an interference between optical signals of a desired signal and an interference, $\langle N_{s_S-s_I}\rangle$, another is one between optical signals of two interferences, $\langle N_{s_I-s_I}\rangle$ and they will be derived in Appendix A.

Therefore, the CINR(carrier-to-interference-plus-noise ratio) of the regenerated radio signal is given by

$$CINR=\frac{C}{I+N}. \tag{4.33}$$

4.4 Numerical Results and Discussions

In this section, we show some numerical results and discussions. Table 4.1 shows parameters used for calculation. Figure 4.3 shows the relationship between the code length L and the CIR for the proposed OPRC and the unipolar type correlator shown in Fig.4.2 for the optical CDMA radio highway in the case of using PN codes for M=10. In the case of the unipolar type correlator using Maximal length codes and Gold codes, there is no improvement in the CIR though L increases. In this case, it is seen from Eq.(4.24) that the CIR almost equals to $4/(M-1)$ regardless of L. However, it is seen from Eq.(4.18) that in the proposed OPRC, the CIR is improved as the L increases. The results show that PN codes such as Maximal length codes and Gold codes can be applied to the optical CDMA radio highway using the proposed OPRC. However, in the case of the optical CDMA radio highway using the unipolar type correlator, it is seen that PN codes can not be applied and only unipolar orthogonal codes can be applied. Refs.[13]-[15] have reported that the prime code is the best code as a unipolar orthogonal code which can provide the highest CIR. So in the next figure, we compare the number of distinct code sequences which results in the limitation of the number of RBS's connected to the radio highway for Maximal length codes, Gold codes and prime codes.

Figure 4.4 shows the number of distinct code sequences versus the code sequence length L. Gold code sequences are generated by combining a pair of preferred Maximal length sequences using modulo-2 addition if the number of preferred maximal length sequences is at least two [47][49]. On the other hand, in the case of prime codes the number of distinct code sequences is equal to the prime number p for the code sequence length of p^2 [13]. The numbers of distinct code sequences for Maximal length codes and Gold codes are larger than that for prime codes. For example, comparing Maximal length codes and Gold codes of L=32767 with prime codes of p^2=32041, the numbers of distinct code sequences for Maximal length codes and Gold codes are 10 times and 183 times larger than that for prime codes, respectively. Therefore, using the proposed OPRC can assign larger number of distinct code sequences to RBS's in optical CDMA radio highway than using the unipolar type correlator using prime

Table 4.1 Parameters used in calculations

responsivity of PD	α	0.8A/W
PSD of the relative intensity noise	ζ_{RIN}	-152dB/Hz
bandwidth of optical filter	W	1THz
noise temperature	T	300K
load resistance	R_L	50 Ω
spontaneous emission factor of OA	η_{sp}	2.0
quantum efficiency of the OA	η_a	0.5
radio signal frequency	f_{rf}	1.9GHz
radio signal bandwidth	B_{rf}	300KHz
coupling plus insertion loss of OC	L_{oc}	3dB
fiber loss between RBS's	L_f	0.5dB
FWHM of the LD	$\Delta\nu_{LD}$	10MHz
difference of center frequency of the LD	Δ_F	1THz

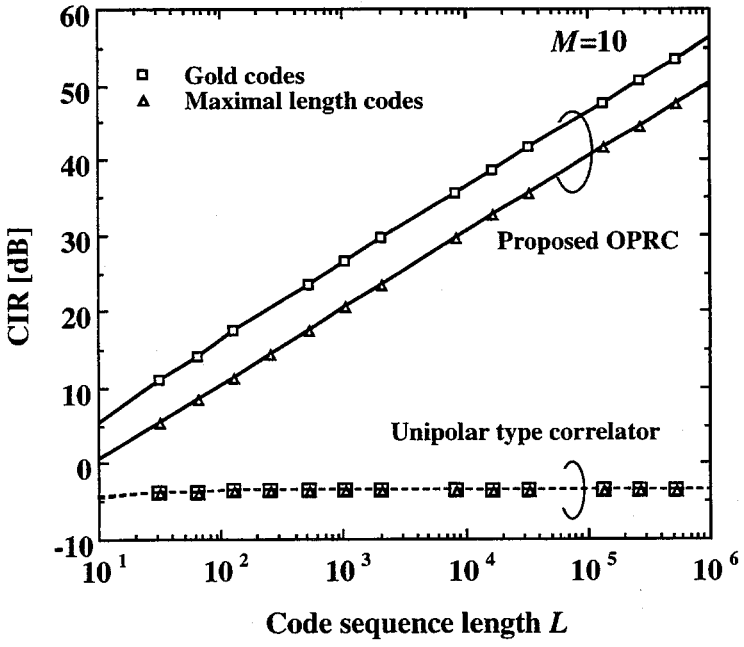

Fig.4.3 Relationship between the code sequence length, L and the CIR.

codes.

Figure 4.5 (a) and (b) show the relationship between the code length L and the CINR in the case of M=30 for P_s of 0dBm and -10dBm, respectively. We calculate the CINR versus L where Gold code sequence is defined. A little better CIR can be obtained by the proposed OPRC using Gold codes than the unipolar type correlator using prime codes. In the case of P_s=0dBm, the CNR in the proposed OPRC using Gold codes is dominated by the optical signal beat noise, $\langle N_{s-s} \rangle$. On the other hand, in the case of the unipolar type correlator using prime codes, the CNR is dominated by the beat noise among ASE of an OA and the optical signal, N_{s-sp}, and deteriorated by the receiver thermal noise, N_{th}, as L comes to large because the carrier power decreases in proportion to 1/L. Thus when radio signal bandwidth, B_{rf} is increased to 900KHz, the CNR is deteriorated by the increase in B_{rf}. When P_s is 0dBm as shown in Fig.4.6 (a), the CINR for the proposed OPRC using Gold codes is dominated by CIR. In the case of the unipolar type correlator using prime codes, the CINR is dominated by CIR until L comes to 262143 from which the CINR is dominated by the CNR of N_{th}. Thus, when P_s is 0dBm, the CINR is a little improved by the proposed OPRC using Gold codes compared with the unipolar type correlator using prime codes because the CIR is determined by the kind of used code sequence.

In the case of P_s=-10dBm as shown in Fig.4.5 (b) , the CNR in the proposed OPRC using Gold codes is dominated by the N_{s-sp}, while in the case of the unipolar type correlator using prime codes, the CNR is dominated by the N_{th} and awfully deteriorated as L comes to large. In the case of the conventional correlator using prime codes, as L increases the CINR is improved by the CIR but deteriorated by the CNR of N_{th} as L increases more than 16383. Thus, in this case, the maximal CINR is determined by the CIR and the CNR. In the case of the small average transmitted optical power such as P_s=-10dBm for the unipolar type correlator using prime codes, it is seen from Fig.4.4 and Fig.4.5 (b) that L should be increased to assign larger number of distinct code sequences to RBS's but the CINR is deteriorated as L comes to large. However, in the case of the proposed OPRC using Gold codes, as the CNR is almost constant regardless of L, the CINR is improved and not deteriorated as L increases.

Figure 4.6 shows the relationship between the average transmitted optical power, P_s and the CINR in the case of M=40 for different switching speeds in the DOS-CDMA, $1/T_c = 2B_{rf}.L$.

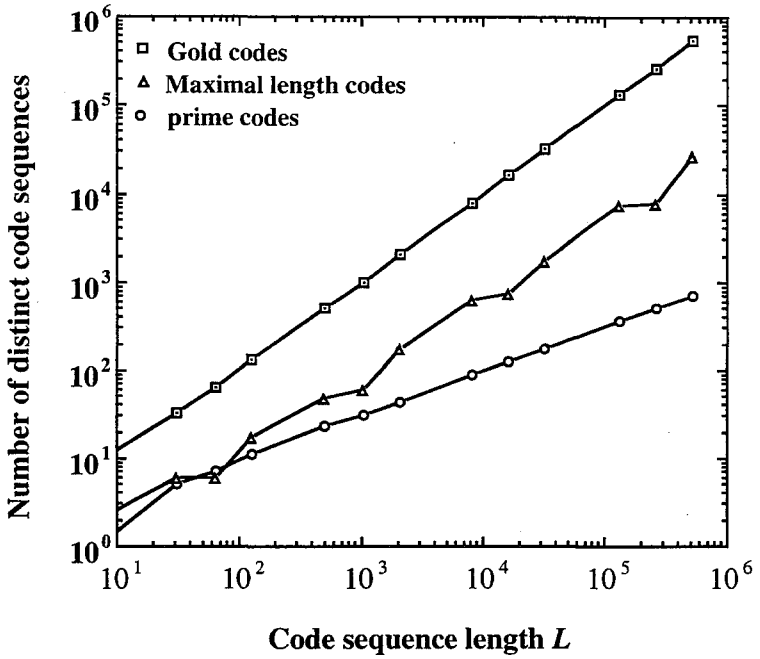

Fig. 4.4 Number of distinct code sequences versus the code sequence length, L.

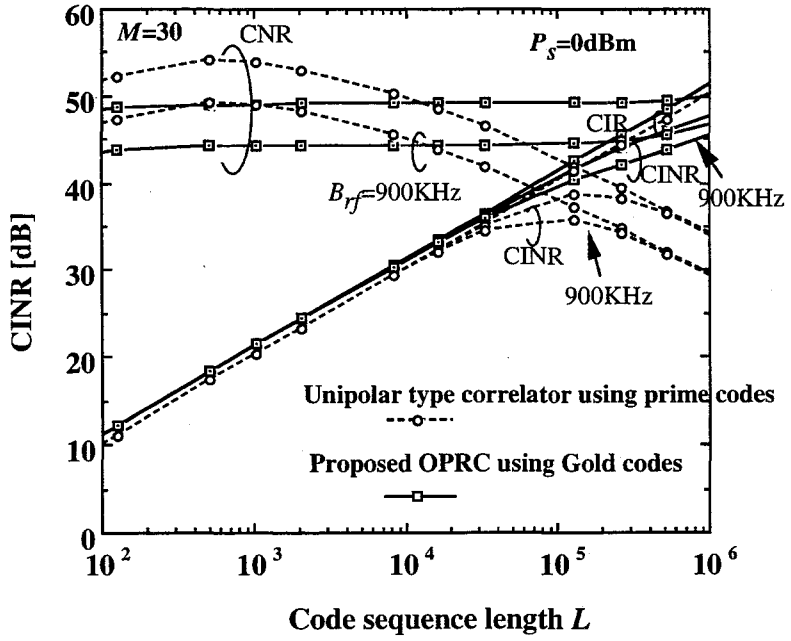

Fig.4.5(a) Relationship between the code sequence length, L and the CINR for P_S=0dBm.

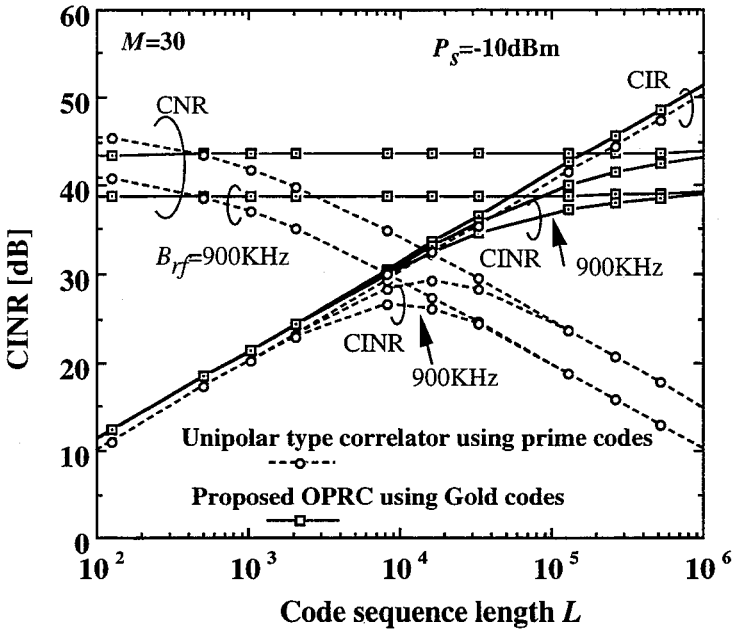

Fig.4.5((b) Relationship between the code sequence length, L and the CINR for -10dBm.

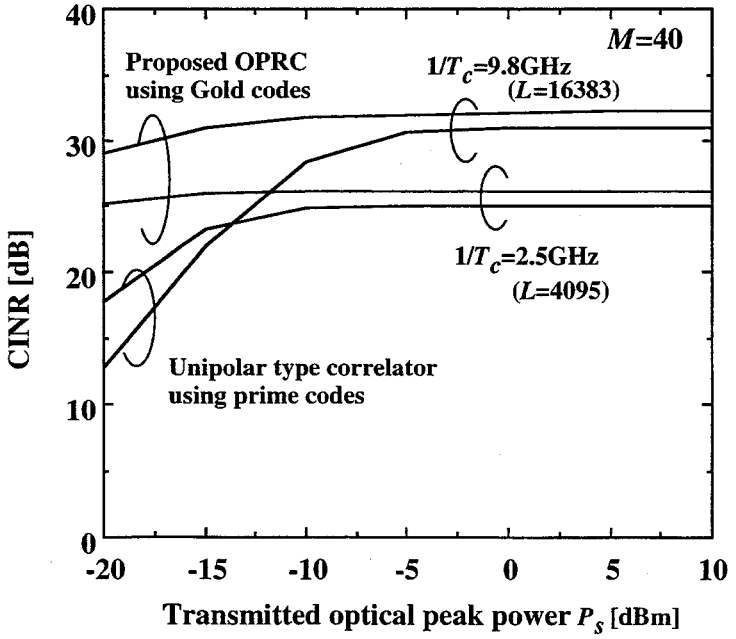

Fig.4.6 Relationship between the average transmitted optical power, P_s and the CINR.

In the unipolar type correlator using prime codes, when $1/T_c$ is large, the CNR dominated by N_{th} awfully deteriorates the CINR as P_s decreases because the signal power is in proportion to $\frac{P_s^2}{L}$. However, in the proposed OPRC using Gold codes, the CINR is not so abruptly deteriorated with the CNR as P_s decreases because the signal power is nearly in proportion to $\frac{P_s^2}{4}$ from Eq. (4.12). Thus, the CINR is more improved by the proposed OPRC using Gold codes compared with the unipolar type correlator using prime codes as P_s decreases.

Figure 4.7 shows the relationship between the switching speed, $1/T_c$, and the number of maximum connected RBS's, $M_{\max}$, in the case that the CINR is 30dB.

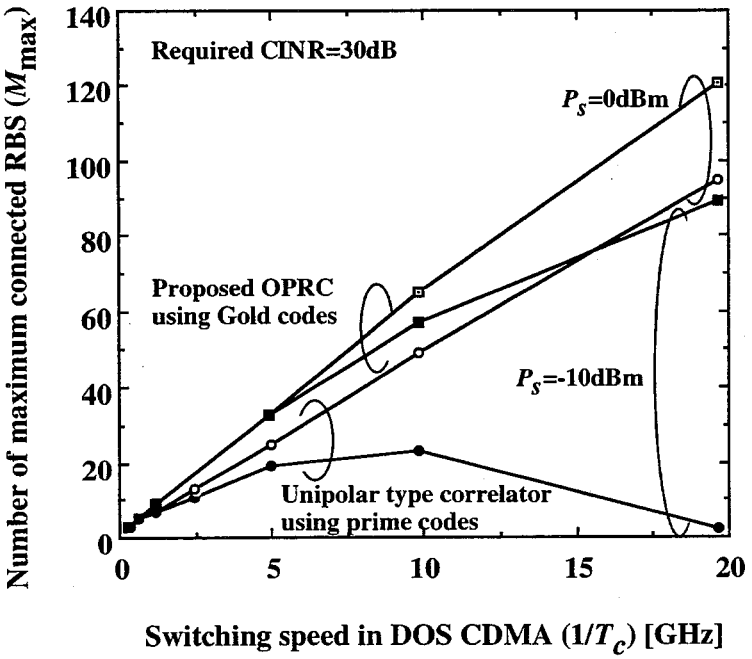

Fig. 4.7 Relationship the switching speed in the DOS-CDMA, $1/T_c$ and the number of maximum connected RBS's, $M_{\max}$.

This figure shows that by the proposed OPRC using Gold codes, the number of maximum connected RBS's can be much more improved for small P_s such as -10dBm compared with the conventional correlator using prime codes. For example, in the case of $1/T_c$= 9.8GHz, by the

proposed OPRC using Gold codes, 1.3 and 2.5 times of RBS's can be accessed to the radio highway with the CINR of 30dB compared with the unipolar type correlator using prime codes for P_s of 0dBm and -10dBm respectively.

4.5 Concluding Remarks

In this chapter, we have newly proposed the optical polarity-reversing correlator(OPRC) for the direct optical switching(DOS) CDMA radio highway network using PN codes such as Maximal length codes and Gold codes which are usually used in radio systems. The carrier-to-interference-plus-noise power ratio(CINR) of the regenerated radio signal at the control station has been theoretically analyzed. The following results are found:

1. We can more assign distinct code sequences to radio base stations connected to the DOS-CDMA radio highway network than the unipolar type correlator using prime codes by using the OPRC with PN codes. For example, comparing Maximal length codes and Gold codes of code length, L=32767 with prime codes of code length, p^2=32041, the numbers of distinct code sequences for Maximal length codes and Gold codes are 10 times and 183 times larger than that for prime codes respectively.
2. For small average transmitted optical powers, the proposed optical polarity reversing correlator using Gold codes can much more improve the number of maximum connected radio base stations than the unipolar type correlator using prime codes. For example, in the case of the switching speed in DOS-CDMA of 9.8GHz, by the proposed OPRC using Gold codes, 1.3 and 2.5 times of radio base stations can be accessed to the DOS-CDMA radio highway network with the CINR of 30dB compared with the unipolar type correlator using prime codes for average transmitted optical powers of 0dBm and -10dBm respectively.

Chapter 5

Reversing Optical Intensity(ROI) CDMA Routing Method for CDMA Radio Systems

5.1 Introduction

In DOS-CDMA methods described in Chapters 3 and 4, as the optical power is zero during the interval of zero parts in prime codes or negative polarity parts in PN codes, the received optical power at the receiver is less than the laser power at the RBS. Also, in order to have the flexibility for conventional CDMA radio systems using all intervals of PN codes, we newly propose the reversing optical intensity(ROI) CDMA method where the spectrum spreading is performed in the optical domain for all intervals of a PN code [40]-[41]. We apply the ROI-CDMA routing scheme to conventional CDMA radio systems in order to route CDM signals to the control station(CS)s , for example, according to services or operators [41]. In the proposed network, at the desired CS the despreading for two-layered spectrum spreading is performed at the optical polarity-reversing correlator (OPRC) by using the code sequence of two-layered spectrum spreading at one time.

5.2 ROI-CDMA Routing Method for CDMA Radio Systems

Figure 5.1 illustrates the configuration of the radio highway using the ROI-CDMA routing method. Radio base station(RBS)s are connected to the fiber-optic bus link, where CDM

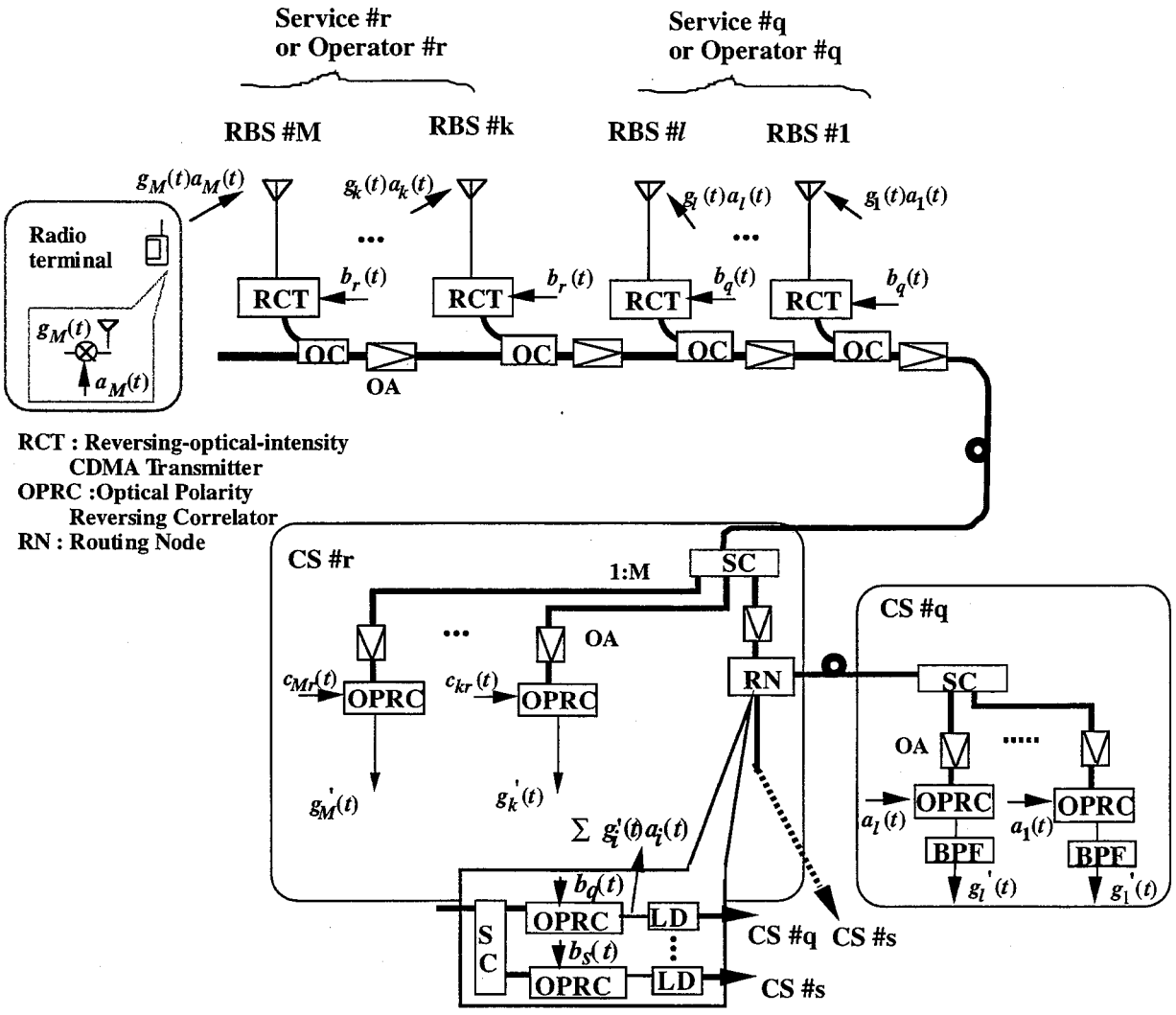

Fig.5.1 Configuration of the radio highway using the ROI-CDMA routing method.

signals from radio terminals are multiplexed by the ROI-CDMA scheme. At the ROI-CDMA transmitter(RCT), the spreading is performed with code sequences such as $b_r(t)$ and $b_q(t)$ used as the routing data of destination CS's according to services or operators. At the bus type fiber link, many IM/CDMA signals are transmitted to the CS. Figure 5.2 illustrates the configurations of the RCT and the optical polarity-reversing correlator (OPRC).

At the receiver of the CS, ROI-CDMA signals from RBS's are at first power-split into OPRC's and the routing node(RN). To compensate the optical loss between RBS and the receiver, each RBS and CS are equipped with OA's. At the k-th OPRC, the average received optical power, P_{r_k}, can be written as Eq.(4.4). It is assumed that the code sequence used in spreading at the RCT and the code sequence of two-layered spectrum spreading are regenerated at the CS by using the retiming code generator such as the retiming block [44]. When the CS is the desired destination CS, namely the code sequence, $b_r(t)$ is regenerated at the CS#r, the despreading for two-layered spectrum spreading is performed at the OPRC at one time and radio signals are regenerated. On the other hand, in the case of routing to other CS's, for example when $b_q(t)$ is regenerated at the CS#r, the despreading is performed at the OPRC by using the code, $b_q(t)$ used in spreading at the RCT, thus CDM signals to the CS#q are regenerated. Regenerated CDM signals are converted into IM signals at the LD and routed to the routing destination CS#q.

5.3 Theoretical Analysis of Carrier-to-Interference-plus-Noise Ratio Performance

The spread spectrum signal received at the k-th RBS, $g_{a_k}(t)$, is written by

$$g_{a_k}(t)=g_k(t)a_k(t), \tag{5.1}$$

where $g_k(t)$ is the radio signal with its bandwidth B_{rf} and carrier frequency f_{rf} and $a_k(t)$ is the PN code with the frame period of T_{F_a}, the chip width of T_{c_a} and the code length of L_a which is the number of chips. In order to simplify the discussion, each RBS receives CDM signals from a radio terminal. $g_{a_k}(t)$ is split in two signals and one of them is phase-shifted by π. Next, two

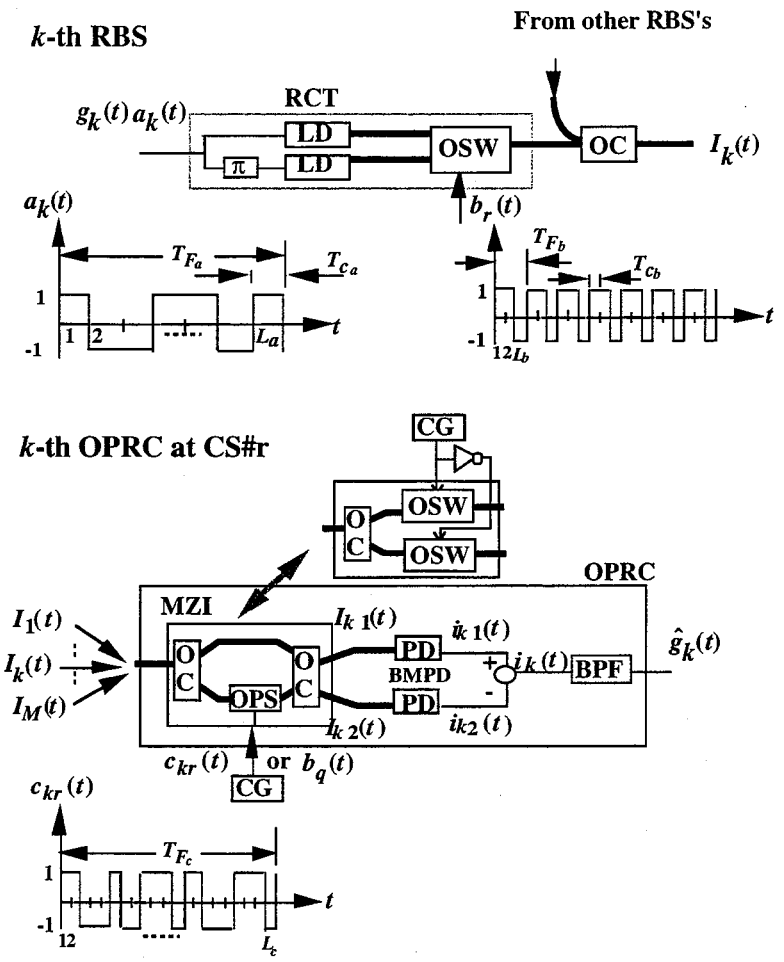

Fig.5.2 Configuration of the RCT and the OPRC.

LD's are directly intensity modulated by them with the optical modulation index of 1. The optical spectrum spreading is performed by switching outputs of two LD's at the OSW according to the polarity of a PN code sequence, $b_r(t)$, having the frame period of T_{F_b}, the chip width of T_{c_b} and the code length of L_b. Code sequences such as $b_r(t)$ and $b_q(t)$ are used as the routing data of destination CS's. It is assumed that the chip synchronization is taken between $a_k(t)$ and $b_r(t)$, T_{c_a} is the integer multiple of T_{c_b} and L_b is less than L_a to simplify the discussion. Thus, $a_k(t)b_r(t)$ can be expressed as $c_{kr}(t)$ having the frame period of T_{F_a},the chip width of T_{c_b} and the code length of L_aL_b. The ROI-CDMA can be expressed as

$$I_k(t)=P_s\{1+g_k(t)a_k(t)b_r(t)\}=P_s\{1+g_k(t)c_{kr}(t)\}. \tag{5.2}$$

At the CS, an OPRC consists of a MZI or two OSW's, a balanced mixing photodetector(BMPD) and a bandpass filter(BPF). Many IM/CDMA signals from many RBS's are received at the MZI which is composed of two OC's and an optical phase shifter(OPS) or two OSW's . It is assumed that an OA equipped at each RBS has the gain G of L_f+L_{oc} and the gain of OA at the output of SC, G_M, is equal to $10\log_{10}M+2L_{oc}$. Thus, each OPRC receives optical signals with the same received power $P_{r_k}=P_s$ $(k=1,2,..,M)$ from Eq.(4.4).

5.3.1 The Desired Destination Control Station

When the CS is the desired destination CS, namely the code sequence, $b_r(t)$ is regenerated at k-th receiver of the CS#r, the k-th OPRC is driven by the PN code, $c_{kr}(t)$. During the positive polarity interval of $c_{kr}(t)$, the phase shift of OPS is set to zero or the upper OSW is set to on , thus IM/CDMA signals are outputted to the upper port of BMPD. During the negative polarity interval of $c_{kr}(t)$, the phase shift of OPS is set to π or the lower OSW is set to on , thus IM/CDMA signals are outputted to the lower port of BMPD. Output currents of the BMPD are expressed as

$$i_{k1}(t)=\alpha \sum_{\substack{j=1 \\ i=q \text{ or } r}}^{M} P_s g_j(t)c_{ji}(t).\frac{1+c_{kr}(t)}{2}+i_{n1}(t), \tag{5.3}$$

$$i_{k2}(t)=\alpha \sum_{\substack{j=1 \\ i=q \text{ or } r}}^{M} P_s g_j(t) c_{ji}(t).\frac{1-c_{kr}(t)}{2}+i_{n2}(t), \tag{5.4}$$

where α is the responsivity of BMPD, and $i_{n1}(t)$ and $i_{n2}(t)$ are additive noise currents, respectively. The input current to the BPF is given by

$$i_k(t)=i_{k1}(t)-i_{k2}(t)=i_{S_k}(t)+i_I(t)+i_N(t), \tag{5.5}$$

where $i_{S_k}(t)$, $i_I(t)$ and $i_N(t)$ are the desired signal, the interference and the additive noise, respectively. $i_{S_k}(t)$ and $i_I(t)$ are expressed as

$$i_{S_k}(t)=\alpha P_s g_k(t), \tag{5.6}$$

$$i_I(t)=\sum_{\substack{j=1, j\neq k \\ i=q \text{ or } r}}^{M} a P_s g_j(t) c_{ji}(t) c_{kr}(t). \tag{5.7}$$

The power spectrum of $i_{S_k}(t)$ is given by

$$S_S(f)=(\alpha P_s)^2 S_g(f), \tag{5.8}$$

where $S_g(f)$ is the power spectrums of $g_k(t)$. We assume that radio signals, $g_j(t)$ $(j=1,2,..,M)$, are nonmodulated carriers which have $S_g(f)$,

$$S_g(f)=\frac{1}{4}\{d(f+f_{rf})+d(f-f_{rf})\}. \tag{5.9}$$

The carrier power at the output of the BPF, C, can be obtained as

$$C=\left\{\int_{f_{rf}-B_{rf}/2}^{f_{rf}+B_{rf}/2}+\int_{-f_{rf}-B_{rf}/2}^{-f_{rf}+B_{rf}/2}\right\} S_S(f)df=\frac{1}{2}(\alpha P_s)^2. \tag{5.10}$$

The autocorrelation of interference is expressed as

$$R_I(\tau)=(M-1)(\alpha P_s)^2 R_g(\tau) R_\gamma(\tau), \tag{5.11}$$

where $R_\gamma(\tau)$ represents the autocorrelation of a function $\gamma_{jk}(t)$ which is defined by $c_{ji}(t)c_{kr}(t)(i=q \text{ or } r)$. $R_\gamma(\tau)$ is given by

$$R_\gamma(\tau)=\overline{a_0^2}+\sum_{k=-\infty, k\neq 0}^{\infty} \frac{1}{L_a L_b}\frac{1}{1+(k\pi/L_a L_b)}\cos\left(\frac{2\pi k\tau}{T_{F_a}}\right), \tag{5.12}$$

where the value of a_0^2 depends on the kind of used code sequences [47]-[49]. The power spectrum of $i_I(t)$ is given by

$$S_I(f)=(M-1)\left(\frac{aP_s}{2}\right)^2 S_g(f)\otimes S_g(f). \tag{5.13}$$

At the output of the BPF, I is obtained as

$$I=\left\{\int_{f_{rf}-B_{rf}/2}^{f_{rf}+B_{rf}/2}+\int_{-f_{rf}-B_{rf}/2}^{-f_{rf}+B_{rf}/2}\right\}S_I(f)df$$

$$=\begin{cases}\dfrac{M-1}{2}(aP_s)^2\dfrac{(L_aL_b)^2+(L_aL_b)-1}{4(L_aL_b)^3}, & \text{for Gold code}\\ \dfrac{M-1}{2}(aP_s)^2\dfrac{(L_aL_b)^2+(L_aL_b)-1}{(L_aL_b)^3}, & \text{for Maximal length code}\end{cases} \tag{5.14}$$

Hence, the carrier-to-interference power ratio(CIR) is written by

$$CIR=\begin{cases}\dfrac{4(L_aL_b)^3}{(M-1)\{(L_aL_b)^2+(L_aL_b)-1\}}, & \text{for Gold codes}\\ \dfrac{(L_aL_b)^3}{(M-1)\{(L_aL_b)^2+(L_aL_b)-1\}}, & \text{for Maximal length codes}\end{cases} \tag{5.15}$$

At the output of BPF, we consider additive noise currents composed of relative intensity noise, shot noise, receiver thermal noise, beat noise between optical signal and amplified spontaneous emission(ASE), beat noise between ASE's and optical signal beat noise. The total noise power, N, is written by

$$N=N_{RIN}+N_{shot}+N_{th}+N_{s-sp}+N_{sp-sp}+\langle N_{s-s}\rangle. \tag{5.16}$$

Each noise power is given by

$$N_{RIN}=\zeta_{RIN}(\alpha P_s)^2 MB_{rf}, \tag{5.17}$$

$$N_{shot}=2e\alpha\left\{P_sM+M(N_{sp}+N_{sp_M})W\right\}B_{rf}, \tag{5.18}$$

$$N_{th}=\frac{8k_BT}{R_L}B_{rf}, \tag{5.19}$$

$$N_{s-sp}=4\alpha^2M^2(N_{sp}+N_{sp_M})P_sB_{rf}, \tag{5.20}$$

$$N_{sp-sp}=2\alpha^2M^2\left(N_{sp}+N_{sp_M}\right)^2\left(W-f_{rf}\right), \tag{5.21}$$

where e, ζ_{RIN}, W, k_B, T and R_L are the electric charge, the PSD of the relative intensity noise, the bandwidth of optical filter at the CS, Boltzmann constant, the noise temperature and the load resistance, respectively [6]. The PSD's of the ASE, N_{sp} and N_{sp_M}, are given by Eq.(4.31) and

(4.32), respectively.

On the other hand, the optical signal beat noise is caused by an interference among M optical carriers from M RBS's is derived in Appendix B.

5.3.2 Routing to Other Control Stations

In the case of routing to other CS's, for example when $b_q(t)$ is regenerated at the CS#r, at the RN the despreading is performed at the OPRC by using the code, $b_q(t)$ used in spreading at the RCT. During the positive polarity interval of $b_q(t)$, the phase shift of OPS is set to zero or the upper OSW is set to on, thus IM/CDMA signals are outputted to the upper port of BMPD. During the negative polarity interval of $b_q(t)$, the phase shift of OPS is set to π or the lower OSW is set to on, thus IM/CDMA signals are outputted to the lower port of BMPD. Output currents of the BMPD are expressed as

$$i_{l1}(t)=\alpha \sum_{\substack{j=1 \\ i=q \text{ or } r}}^{M} P_s g_j(t)a_j(t)b_i(t).\frac{1+b_q(t)}{2}+i_{n1}(t), \tag{5.22}$$

$$i_{l2}(t)=\alpha \sum_{\substack{j=1 \\ i=q \text{ or } r}}^{M} P_s g_j(t)a_j(t)b_i(t).\frac{1-b_q(t)}{2}+i_{n2}(t). \tag{5.23}$$

The input current to the BPF is given by

$$\begin{aligned} i_l(t)&=i_{l1}(t)-i_{l2}(t) \\ &=\alpha P_s \sum_{j=1}^{R} g_j(t)a_j(t)+\alpha P_s \sum_{j=R+1}^{M} g_j(t)a_j(t)b_r(t)b_q(t)+i_N, \end{aligned} \tag{5.24}$$

where R is the RBS number routed to CS#q out of M RBS's.

5.4 Numerical Results and Discussions

Some numerical results are discussed below with parameters indicated in Table 4.1. Fig.5.3 shows the relationship between the CIR and the code sequence length L_a in the domain of electrical signal for CDMA radios in the case of the RBS number of 30 and using Maximal

codes. In the proposed ROI-CDMA radio highway, the process gain can be more gained by increasing the code sequence length L_b at the RCT compared with the radio highway using the electrical CDMA and IM method. Thus, it is seen from this figure that in the proposed ROI CDMA radio highway, the CIR is more improved by increasing the code sequence length L_b at the RCT than the radio highway using the electrical CDMA and IM method.

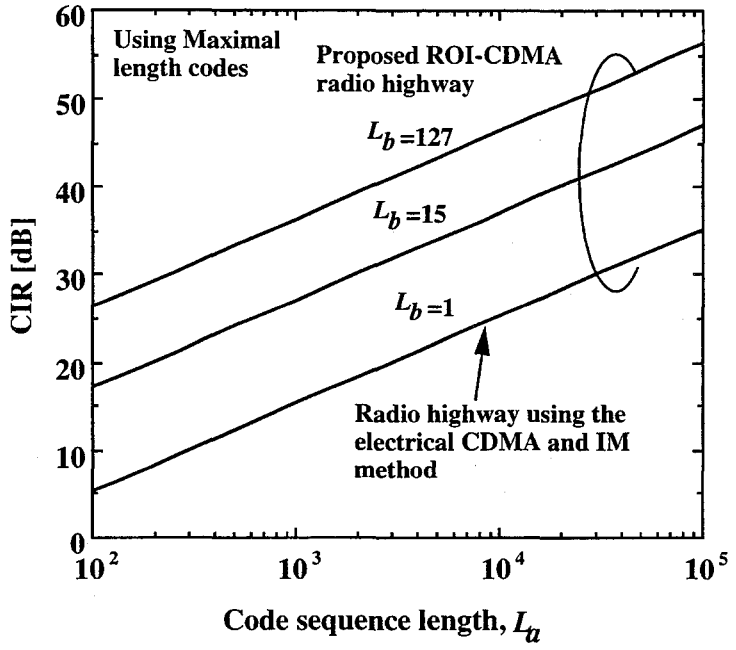

Fig.5.3 Relationship between the CIR and the code sequence length, L_a.

Fig.5.4 shows the relationship between the CNR and the code sequence length L_a in the domain of electrical signal for CDMA radios in the case of the RBS number of 30. In the radio highway using the electrical CDMA and IM method, the CNR is dominated by the optical signal beat noise, $\langle N_{s-s} \rangle$[15]. On the other hand, in the case of the ROI-CDMA radio highway, $\langle N_{s-s} \rangle$ is reduced by the subtraction process and the BPF at the OPRC and the CNR is dominated by the beat noise among ASE of an OA and the optical signal, N_{s-sp}. In the case of the CDMA radio highway with the OC bus connection, the CNR is more deteriorated by $\langle N_{s-s} \rangle$ than N_{s-sp} [12].

Therefore, it is seen from this figure that the CNR in the ROI-CDMA radio highway is improved compared with the radio highway using the electrical CDMA.

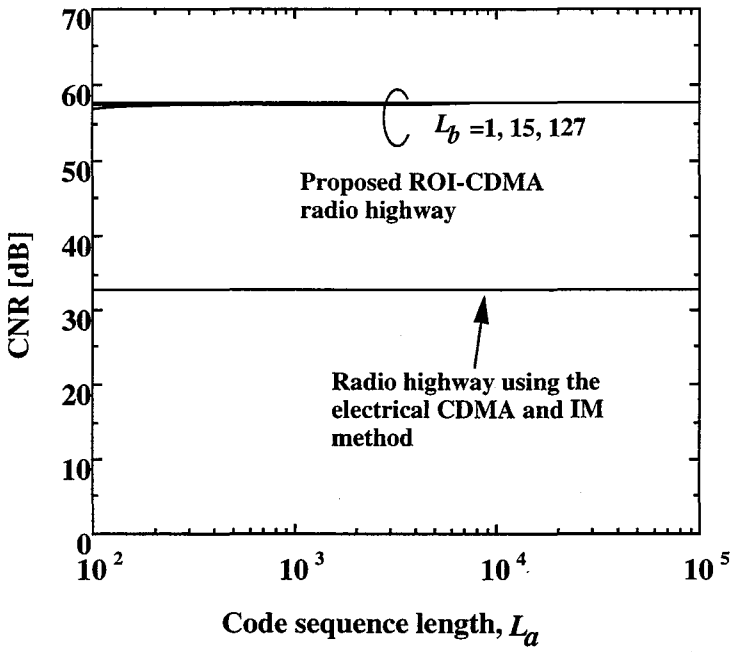

Fig.5.4 Relationship between the CNR and the code sequence length, L_a.

Fig.5.5 shows the relationship between the CINR and the code sequence length L_a in the domain of electrical signal for CDMA radios in the case of the RBS number of 30 and using Maximal codes. In the radio highway using the electrical CDMA and IM method, the CINR is dominated by the CIR for the small value of L_a and by the CNR as L_a increases. On the other hand, in the proposed ROI- CDMA radio highway, the CINR is dominated by the CIR. Thus, it is seen from this figure that in the proposed ROI CDMA radio highway, the CINR is more improved by increasing the code sequence length L_b at the RCT than that in the radio highway using the electrical CDMA and IM method.

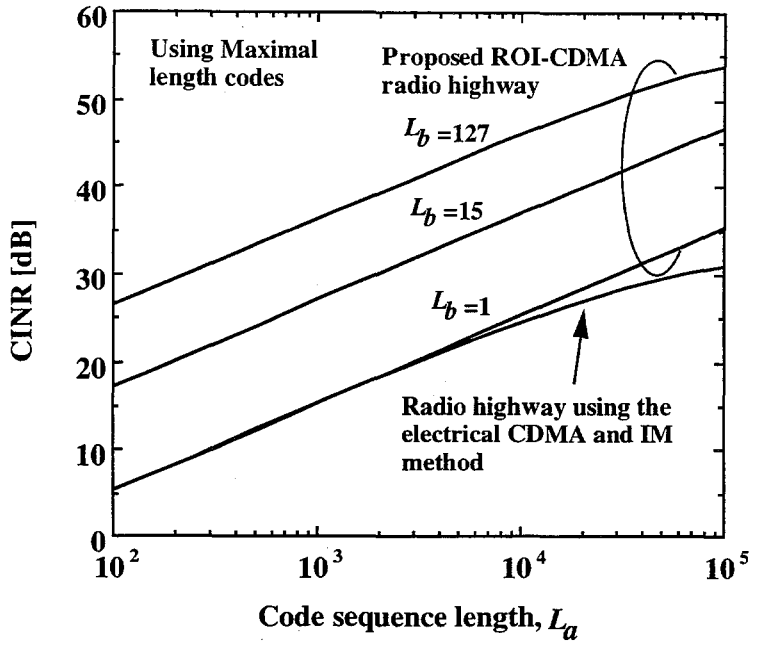

Fig.5.5 Relationship between the CINR and the code sequence length, L_a.

5.5 Concluding Remarks

In this chapter, we have newly proposed the reversing optical intensity(ROI) CDMA method where spectrum spreading is performed during all intervals of a PN code in order to increase the received optical power at the receiver and have the flexibility for conventional CDMA radio systems. We have applied the ROI-CDMA routing scheme to conventional CDMA radio systems in order to route CDM signals to the control station according to services or operators. In the proposed network, at the desired control station the despreading for two-layered spectrum spreadings is performed at the optical polarity-reversing correlator (OPRC) by using the code sequence of two-layered spectrum spreadings at one time. It is found that the carrier-to-interference-plus-noise power ratio can be more improved by increasing the code sequence

length at the ROI-CDMA transmitter than that in the radio highway using the electrical CDMA and intensity modulation(IM) method.

Chapter 6
Conclusions

In this thesis, optical code division multiple access(CDMA) methods have been proposed for fiber-optic radio highway networks from the view points of the flexibility in assigning code sequences and the optical CDMA using intensity modulation. The followings are the conclusions obtained from Chapter 2- Chapter 5 in this study.

1. We have described the various types of multiple access methods for fiber-optic radio networks and performed the comparison of these methods. Also we have described the conventional optical CDMA methods and discussed the necessity for a new type of optical CDMA method for fiber-optic radio highway networks.
2. We have investigated the direct optical switching(DOS) CDMA method for fiber-optic radio networks including cable-to-the-air(CATA) systems where the concept of fiber-to-the-air (FTTA) is applied to cable TV(CATV) systems. The configuration of the DOS-CDMA CATA system has been proposed by using the optical coupler and the optical switch connections. We have theoretically analyzed the carrier-to-interference-plus-noise power ratio(CINR)s of regenerated radio signals at the head end for two types of bus connection methods considering the chip pulse erasure at the optical switch. It is found that in the optical switch connection system, by introducing the additional optical gain at each radio base station, the carrier-to-interference power ratios for all radio base stations can be almost the same as those in the prime code number increases more than the number of connected radio base stations. It is also found that in the optical switch connection system with the additional gain, CINR's for all radio base station(RBS)s and the number of connected radio base stations can be improved compared with the optical coupler connection system.

For example, by using the optical switch connection system with the additional optical gain, G_a=0.2dB, three times of radio base stations can be connected to the CATA system with the CINR of 30dB and the average received optical power from the farthest RBS normalized by the average transmitted optical power of 20dB for the prime number of 79, compared with the optical coupler connection system. Thus the optical switch connection is an effective DOS-CDMA CATA system where an optical switch is used not only to spread the spectrum of optical signals but also to launch them into the fiber-optic bus link.

3. We have newly proposed the optical polarity-reversing correlator(OPRC) for DOS-CDMA radio highway networks using PN codes such as Maximal length codes and Gold codes which are usually used in radio systems. It is found that we can more assign distinct code sequences to radio base stations connected to DOS-CDMA radio highway networks than the unipolar type correlator using prime codes by using the OPRC with PN codes. For example, comparing Maximal length codes and Gold codes of code length, L=32767, with prime codes of code length, p^2=32041, the numbers of distinct code sequences for Maximal length codes and Gold codes are 10 times and 183 times larger than that for prime codes respectively. It is also found that for small average transmitted optical powers, the proposed OPRC using Gold codes can much more improve the number of maximum connected radio base stations than the unipolar type correlator using prime codes. For example, in the case of the switching speed in DOS-CDMA of 9.8GHz by the proposed OPRC using Gold codes, 1.3 and 2.5 times of radio base stations can be accessed to DOS-CDMA radio highway networks with the CINR of 30dB compared with the unipolar type correlator using prime codes for average transmitted optical powers of 0dBm and -10dBm respectively.
4. We have newly proposed the reversing optical intensity(ROI) CDMA method where the spectrum spreading is performed for all intervals of a PN code in order to increase the received optical power at the receiver and have the flexibility for conventional CDMA radio systems. We have applied the ROI-CDMA routing scheme to conventional CDMA radio systems to route CDM signals to the control station according to services or operators. In the proposed network, at the desired control station the despreading for two-layered spectrum spreadings is performed at the OPRC by using the code sequence of two-layered spectrum

spreadings at one time. It is found that the CINR can be more improved by increasing the code sequence length at the ROI-CDMA transmitter than that in the radio highway network using the electrical CDMA and intensity modulation(IM) method.

References

[1] A. Baier, U.C. Fiebig, W. Koch, P. Teder, and J. Thielecke, "Design study for a CDMA-based third generation mobile radio system", IEEE J. of Selected Area in Commun. vol.12, no.4, pp.733-743, May 1994.

[2] K. Pahlavan, A. Zahedi, and P. Krishnamurthy, "Wideband local access: wireless LAN and wireless ATM", IEEE Commun. Mag., pp.35-40, Nov. 1997.

[3] Y. H. Chang, D. Coggins, D. Pitt, D. Skellern, M. Thapar and C. Venkatraman, "An open-systems approach to video on demand", IEEE Commun. Mag., pp.69-80, May. 1994.

[4] T. Yoshida, "A high speed wireless access link-solution of last mile problems", Proc. of Microwave workshops and exhibition(MWE), pp195-200, Sept. 1993.

[5] D. C. Cox, "A radio system proposal for widespread low-power tetherless communications", IEEE Trans. on Commun., vol.39, no.2, pp.324-335, Feb. 1991.

[6] T. Fujii, K. Tsukamoto, and N. Morinaga, "Transmission characteristics anlysis of optical fiber bus link with optical amplifier for microcellular communication systems", IEICE Tech. Report, RCS92-76, pp43-48, Oct. 1992.

[7] K.Tsukamoto, H. Harada, S. Kajiya, and S. Komaki, "TDM intercell connection fiber-optic bus link for personal radio communication systems", Proc. of APMC'94, pp1039-1042, Dec. 1994.

[8] S. Komaki, K. Tsukamoto, S. Hara, and N. Morinaga, "Proposal of fiber and radio extension link for future personal communications", Microwave and optical technology letters, vol.6, no.1, pp55-60, Jan. 1993.

[9] S. Komaki, K. Tsukamoto, M. Okada, and H. Harada, "Proposal of radio highway networks for future multimedia-personal wireless communications", Proc. of ICPWC'94, pp.204-208, Aug. 1994.

[10] H. Yanikomeroglu and E. S. Sousa, "Antenna interconnection strategies for personal communication systems", IEEE J. of Select. Areas Commun., vol.15, no.7, pp1327-1336, Sep. 1997.

[11] T. H. Wood and N. K. Shankaranarayanan, "Operation of a passive optical network with subcarrier multiplexing in the presence of optical beat interference", IEEE J. of Lightwave Tech., vol.LT-11, pp1632-1640, Oct. 1993.

[12] S. Kajiya,H. Harada, K.Tsukamoto, and S. Komaki, "TDM optical fiber bus link for microcellular radio communication system", Proc. IEICE Spring Conf., B-325, p2-325, Mar. 1994.

[13] H. Harada, S. Kajiya, K.Tsukamoto, and S. Komaki, "TDM intercell connection fiber-optic bus link for personal radio communication systems", IEICE Trans. Commun., vol.E78-B, no.9, pp1287-1294, Sep. 1995.

[14] M. M. Banat and M. Kavehrad, "Reduction of optical beat interference in SCM/WDM networks using pseudorandom phase modulation", IEEE J. of Lightwave Tech., vol.LT-12, No.10, pp1863-1868, Oct. 1994.

[15] S. Kajiya, K. Tsukamoto, and S. Komaki, "Proposal of fiber-optic radio highway networks using CDMA method", IEICE Trans. Electronics, vol.E79-C, no.1, pp111-117, Jan. 1996.

[16] P. R. Prucnal, M. A. Santoro, and T. R. Fan, "Spread spectrum fiber-optic local area network using optical processing", IEEE J. of Lightwave Tech., vol.LT-4, no.5, pp547-554, May 1986.

[17] P. R. Prucnal, M. A. Santoro, and S. K Sehgal, "Ultrafast all optical synchronous multiple access fiber networks", IEEE J. on Select. area in Commun., vol.SAC-4, no.9, pp1484-1493, Dec. 1986.

[18] M. A. Santoro and P. R. Prucnal, "Asynchronous fiber optic local area network using CDMA and optical correlation", Proc. IEEE , vol.79, No.9, pp1336-1338, Sept. 1987.

[19] W. C. Kwong, P. A. Perrier, and P. R. Prucnal, "Performance comparison of asynchronous and synchronous CDMA techniques for fiber-optic local area networks", IEEE Trans. Commun., vol.39, no.11, pp1625-1634, Nov. 1991.

[20] A. S. Holmes and R. R. A. Syms, "Al optical CDMA using Quasai-Prime codes", IEEE J.

of Lightwave Tech., vol.LT-10, no.2, pp279-286, Feb. 1992.

[21] J. A. Salehi, A. M. Weiner, and J. P. Heritage, "Coherent ultrashot light pulse code-division multiple access communication systems", IEEE J. of Lightwave Tech., vol.7, no.3, pp478-491, Mar. 1990.

[22] D. Zaccarin and M. Kavehrad, "All optical CDMA system based on spectral encoding of LED", IEEE Photon. Tech. Lett., vol.4, no.4, pp479-482, Apr. 1993.

[23] S. Benedetto and G. Olmo, "Performance evaluation of coherent optical CDMA", Electronics Letter, vol.27, no. 22, pp2000-2002, Oct. 1991.

[24] G.J. Foschini and G. Vannucci, "Using spread-spectrum in a high-capacity fiber-optical network", IEEE J. of Lightwave Tech., vol.LT-6, no.3, pp370-379, Mar. 1988.

[25] G. Vannucci and S. Yang, "Experimental spreading and despreading of the optical spectrum", IEEE Trans. Commun., vol.37, no.1, pp63-65, Jan. 1994.

[26] J. A. Salehi, "Code division multiple access techniques in optical fiber networks-parts I:fundamental principles", IEEE Trans. Commun., vol.E37, no.8, pp824-833, Aug. 1989.

[27] S.J. Park, K. Tsukamoto, and S. Komaki, "Proposal of CDMA cable-to-the air system", Proc. IEICE Spring Conf., SB-5-8, pp.665-666, Mar. 1996.

[28] S.J. Park, K. Tsukamoto, and S. Komaki, "Multimedia mobile radio highway networks using optical CDMA multiplexing method", Proc. MDMC(Multidimensional Mobile Communications), Korea, pp.838-841, July 1996.

[29] S.J. Park, K. Tsukamoto, and S. Komaki, "Proposal of direct optical switching CDMA for cable-to-the-air system and its performance analysis", IEICE Trans. on Commun. vol. E81-B, no.6, pp1188-1196, June 1998.

[30] S.J. Park, K. Tsukamoto, and S. Komaki, "performance analysis of Direct Optical Switching CDMA Cable-To-The-Air network", Proc. SPIE(International Society for Optical Engineering) optical fiber communication, 3420-04, Taiwan, pp.20-29, Jul. 1998.

[31] T. O'Farrell and S. I. Lochmann, "Performance analysis of an optical correlator receiver for SIK DS-CDMA communication systems", Electron. Letters, vol.30, no.1, pp.63-65, Jan. 1994.

[32] T. O'Farrell and S. I. Lochmann, "Switched correlator receiver architecture for optical

CDMA networks with bipolar capacity", Electron. Letters, vol.31, no.11, pp.905-906, May 1995.

[33] F. Khaleghi and M. Kavehrad, "A new correlator receiver architecture for noncoherent optical CDMA networks with bipolar capacity", IEEE Trans. on Commun.,vol.44, no.10, pp.1335-1339, Oct. 1996.

[34] L. Nguyen, B. Aazhang and J. F. Young, "All-optical CDMA with bipolar codes", Electron. Letters, vol.31, no.6, pp.469-470, Mar. 1995.

[35] S.J. Park, K. Tsukamoto, and S. Komaki, "Proposal of radio highway network using a novel Direct Optical Switched CDMA method", Proc. MWP(Microwave Photonics), TU4-6, Japan, pp.77-80, Dec. 1996.

[36] S.J. Park, K. Tsukamoto, and S. Komaki, "Radio highway networks using optical CDMA with optical polarity reversed correlator", Proc. MWP(Microwave Photonics), FR2-3, Germany, pp.227-230, Sep. 1997.

[37] S.J. Park, K. Tsukamoto, and S. Komaki, "Polarity-reversing type photonic receiving scheme for optical CDMA signal in radio highway", IEICE Trans. on Electron. vol. E81-C, no.3, pp462-467, March 1998.

[38] S.J. Park, K. Tsukamoto, and S. Komaki, "Proposal of radio highway networks using optical DOS-CDMA method", IEICE Tech. Report, OMI96-8, pp.39-44, July 1996.

[39] S.J. Park, K. Tsukamoto, and S. Komaki, "Theoretical analysis on connectable RBS number and CNR in direct optical switching CDMA radio highway", IEICE Tech. Report, MWP97-23, pp.80-85, Jan. 1998.

[40] S. J. Park, K. Tsukamoto, and S. Komaki, "Proposal of reversing optical intensity type DOS-CDMA radio highway", Proc. IEICE Autumn Conf., B-500, p.501, Sept. 1996.

[41] S.J. Park, K. Tsukamoto, and S. Komaki, "Proposal of reversing optical intensity CDMA routing method in radio highway for CDMA radio", Proc. CIC(CDMA international conference), Korea, pp269-272, Oct. 1998.

[42] T. L. Duffield, "A comparison of modulation techniques for quantized voice communications", IEEE Trans. Commun., vol.18, no.5, pp543-550, Oct. 1970.

[43] A. Kohlenberg, "Exat Interpolation of Band-Limited Functions", J. of applied physics,

vol.12, no.12, pp1432-1436, Dec. 1953.

[44] T. Onoda and N. Miki, "Bidirectional multiplexing for optical subscriber systems using code division multiplexing", IEICE Trans. on Commun. vol. J76-B, no.8, pp629-642, Aug. 1993.

[45] A. A. Shaar and P. A. Davies, "Prime sequences:Quasi-optimal sequences for or channel code division multiplexing", Electronics Letter, vol.19, no. 21, pp888-889, Oct. 1983.

[46] K.Tsukamoto, T. Fujii and N. Morinaga, "Multiaccess coherent optical communication system using common optical carrier with star configuration", IEICE Trans. Commun., Vol.J77-B-I, No.5, pp267-274, May 1994.

[47] M. Yokoyama, "Spectrum spreading communication system", Science technology Inc., pp.401-409,1988.

[48] M. Yokoyama, "performance analysis of a SSRA communication system", IEICE Trans. on Commun., vol.J64-B, no.1, pp.16-23, Jan. 1981.

[49] S. Tamura, S. Nakano, and K. Okazaki, "Optical code-multiplex transmission by Gold sequence", J. of Lightwave Tech., vol.LT-3, no.1, pp.121-127, Feb. 1985.

Appendix

Appendix A. Optical Signal Beat Noise for DOS-CDMA Radio Networks Using OPRC

Optical carrier signals of a desired signal from the j-th RBS at the upper and the lower ports of the k-th MZI, $f_{1j}(t)$ and $f_{2j}(t)$, can be written as

$$f_{1j}(t)=\left[P_s g_j(t)c_j(t).\frac{1+c_k(t)}{2}\right]^{1/2}\mathrm{Re}\left[e^{j\{2\pi f_{oj}t+\phi_j(t)\}}\right]\ j=1,2,..,M, \tag{A.1}$$

$$f_{2j}(t)=\left[P_s g_j(t)c_j(t).\frac{1-c_k(t)}{2}\right]^{1/2}\mathrm{Re}\left[e^{j\{2\pi f_{oj}t+\phi_j(t)+\pi\}}\right]j=1,2,..,M, \tag{A.2}$$

where f_{oj} is the center frequency of LD and $\phi_j(t)$ is the phase component of optical carrier at the j-th RBS. At first, we consider the beat noise caused by an interference between optical signals of a desired signal and an interference signal, $\langle N_{s_S-s_I}\rangle$. The current of beat noise between desired signal and interference at the input of BPF, $i_{s_S-s_I}(t)$, is given by

$$\begin{aligned} i_{s_S-s_I}(t)&=\sum_{j=1,j\neq k}^{M}\left[\frac{\alpha}{2}\left|f_{1k}(t)f_{1j}^{*}(t)\right|-\frac{\alpha}{2}\left|f_{2k}(t)f_{2j}^{*}(t)\right|\right]\\ &=\sum_{j=1,j\neq k}^{M}\frac{\alpha P_s}{2}\left[g_j(t)g_k(t)\right]^{1/2}\mathrm{Re}\left[e^{j\{2\pi\Delta f_{kj}t+\phi_k(t)-\phi_j(t)\}}\right]a(t), \end{aligned} \tag{A.3}$$

where $\Delta f_{kj}=f_{ok}-f_{oj}$ and $a(t)=\frac{1+c_j(t)}{2}.\frac{1+c_k(t)}{2}$.

The PSD of $a(t)$, $S_a(f)$, can be written as

$$\begin{aligned} S_a(f)=\left(\frac{1}{4}\right)^2\Bigg[&\left\{1+\frac{4}{L}+\frac{4}{L^2}+\frac{2(L+2)}{L^3}+\overline{a_0^2}\right\}\delta(f)\\ &+\sum_{m=-\infty,m\neq 0}^{\infty}\left\{\frac{2(L+1)(L+2)}{L^3}\mathrm{sinc}^2\left(\frac{\pi m}{L}\right)+\frac{1}{L}\frac{1}{1+(m\pi/L)}\right\}\delta(f-2B_{rf}m)\Bigg], \end{aligned} \tag{A.4}$$

It is assumed that the DOS-CDMA signal has a single mode gaussian shaped spectrum with the full width half maximum(FWHM) after DOS-CDMA driven by the biased bipolar code, Δν, given by

$$\Delta\nu=\sqrt{\Delta\nu_{LD}+\left(LB_{rf}\right)^2}\,, \tag{A.5}$$

where $\Delta\nu_{LD}$ is the FWHM of the LD [6][15]. The PSD of $i_{sS-sI}(t)$, $S_{sS-sI}(f)$, can be written as

$$\begin{aligned} S_{sS-sI}(f)=&\left(\frac{\alpha P_s}{4}\right)^2\left\{1+\frac{4}{L}+\frac{4}{L^2}+\frac{2(L+2)}{L^3}+\overline{a_0^2}\right\}\sum_{j=1,j\neq k}^{M}\left\{\frac{1}{2\sigma\sqrt{2\pi}}e^{-\frac{(f-\Delta f_{jk})^2}{2\sigma^2}}\right.\\ &\left.+\frac{1}{2\sigma\sqrt{2\pi}}e^{-\frac{(f+\Delta f_{jk})^2}{2\sigma^2}}\right\}+\sum_{m=-\infty,m\neq 0}^{\infty}\left\{\frac{2(L+1)(L+2)}{L^3}\mathrm{sinc}^2\left(\frac{\pi m}{L}\right)\right.\\ &\left.+\frac{1}{L}\frac{1}{1+(m\pi/L)}\right\}\sum_{j=1,j\neq k}^{M}\left\{\frac{1}{2\sigma\sqrt{2\pi}}e^{-\frac{(f-2B_{rf}m-\Delta f_{jk})^2}{2\sigma^2}}\right.\\ &\left.+\frac{1}{2\sigma\sqrt{2\pi}}e^{-\frac{(f-2B_{rf}m+\Delta f_{jk})^2}{2\sigma^2}}\right\}, \end{aligned} \tag{A.6}$$

where

$$\sigma=\frac{\Delta\nu}{2\log 2} \tag{A.7}$$

The $S_{sS-sI}(f)$ appears in the radio frequency band after the photodetection, but its frequency location depends on the frequency difference among LD's of M RBS's. So we treat its power N_{sS-sI} as a random variable and derive its average power $\langle N_{sS-sI}\rangle$. At the output of the BPF, N_{sS-sI} is given by

$$\begin{aligned} N_{sS-sI}=&\left(\frac{\alpha P_s}{4}\right)^2\left\{1+\frac{4}{L}+\frac{4}{L^2}+\frac{2(L+2)}{L^3}+\overline{a_0^2}\right\}\sum_{j=1,j\neq k}^{M}\left[erfc\left\{\frac{-2(f_{rf}+\Delta f_{jk})-B_{rf}}{2\sqrt{2}\sigma}\right\}\right.\\ &-erfc\left\{\frac{-2(f_{rf}+\Delta f_{jk})+B_{rf}}{2\sqrt{2}\sigma}\right\}+erfc\left\{\frac{-2(f_{rf}-\Delta f_{jk})-B_{rf}}{2\sqrt{2}\sigma}\right\}\\ &\left.-erfc\left\{\frac{-2(f_{rf}-\Delta f_{jk})+B_{rf}}{2\sqrt{2}\sigma}\right\}\right]. \end{aligned} \tag{A.8}$$

Assuming that optical carrier frequencies at RBS's, f_{oj} ($j=1,2,...,M$) are mutually independent random variables with its mean of f_0 and a uniform probability density function(PDF) in the range of $|f_{oj}-f_0|<\Delta F/2$ [6], the PDF of Δf_{kj}, $p(\Delta f_{kj})$, is given by

$$p(\Delta f_{kj})=\begin{cases}\frac{1}{(\Delta F)^2}(\Delta F-|\Delta f_{kj}|); \Delta f_{kj}\le\Delta F \\ 0 \qquad\qquad\qquad ; \Delta f_{kj}>\Delta F\end{cases} (j,k=1,2,..,M, j\neq k). \tag{A.9}$$

The ensemble average of $N_{s_S-s_I}$, $\langle N_{s_S-s_I}\rangle$, is given by

$$\langle N_{s_S-s_I}\rangle=\int_{-\Delta F}^{\Delta F} N_{s_S-s_I}\, p(\Delta f_{kj})\, d\Delta f_{kj}. \tag{A.10}$$

The beat noise caused by an interference between optical signals of two interferences, $\langle N_{s_I-s_I}\rangle$ is examined. The current of beat noise between two interferences at the input of BPF, $i_{s_I-s_I}(t)$, is given by

$$\begin{aligned} i_{s_I-s_I}(t) &= \sum_{i=1,i\neq k}^{M}\sum_{j=1,j\neq i}^{M}\left[\frac{\alpha}{2}\left|f_{1j}(t)f_{1i}^{*}(t)\right|-\frac{\alpha}{2}\left|f_{2j}(t)f_{2i}^{*}(t)\right|\right] \\ &= \sum_{i=1,i\neq k}^{M}\sum_{j=1,j\neq i}^{M}\frac{\alpha P_s}{2}\left[g_i(t)g_j(t)\right]^{1/2}\mathrm{Re}\left[e^{j\{2\pi\Delta f_{ji}t+\phi_j(t)-\phi_i(t)\}}\right]b(t), \end{aligned} \tag{A.11}$$

where $b(t)=\frac{1+c_i(t)}{2}\cdot\frac{1+c_j(t)}{2}c_k(t)$ and $\Delta f_{ji}=f_{oj}-f_{oi}$. The autocorrelation of $b(t)$, $R_b(\tau)$, is expressed as

$$R_b(\tau)=\left(\frac{1}{4}\right)^2\left\{R_c(\tau)\left(\frac{L+2}{L}\right)^2+2R_\gamma(\tau)\frac{L+2}{L}+R_\beta(\tau)\right\}, \tag{A.12}$$

where $R_\beta(\tau)$ represents the autocorrelation of $c_i(t).c_j(t).c_k(t)$. As the ensemble of the square of $c_i(t).c_j(t).c_k(t)$ is approximately calculated as $1/L$ [48] , its auto correlation, $R_\beta(\tau)$, can be given by

$$R_\beta(\tau)\simeq\frac{1}{L}+\sum_{k=-\infty,k\neq 0}^{\infty}A(L)\cos\left(\frac{2\pi k\tau}{T_F}\right), \tag{A.13}$$

where $A(L)$ is a function of L.

The PSD of $b(t)$, $S_b(f)$, can be written as

$$S_b(f)\approx\left(\frac{1}{4}\right)^2\left\{\frac{1}{L^2}\left(\frac{L+2}{L}\right)^2+2\frac{L+2}{L}\overline{a_0^2}+\frac{1}{L}\right\}\delta(f)$$
$$+\left(\frac{1}{4}\right)^2\sum_{m=-\infty,m\neq 0}^{\infty}\left\{\left(\frac{L+2}{L}\right)^2\frac{L+1}{L^2}\mathrm{sinc}^2\left(\frac{\pi m}{L}\right)+\frac{2L+4}{L^2}\frac{1}{1+(m\pi/L)}+A(L)\right\}\delta(f-2B_{rf}m)\Bigg]. \quad \text{(A.14)}$$

The PSD of $i_{s_I-s_I}(t)$, $S_{s_I-s_I}(f)$, can be written as

$$S_{s_I-s_I}(f)=\left(\frac{\alpha P_s}{4}\right)^2\left\{\frac{1}{L^2}\left(\frac{L+2}{L}\right)^2+2\frac{L+2}{L}\overline{a_0^2}+\frac{1}{L}\right\}\sum_{i=1,i\neq k}^{M}\sum_{j=1,j\neq i}^{M}\left\{\frac{1}{2\sigma\sqrt{2\pi}}e^{-\frac{(f-\Delta f_{ji})^2}{2\sigma^2}}\right.$$
$$\left.+\frac{1}{2\sigma\sqrt{2\pi}}e^{-\frac{(f+\Delta f_{ji})^2}{2\sigma^2}}\right\}+\sum_{m=-\infty,m\neq 0}^{\infty}\left(\frac{\alpha P_s}{4}\right)^2\left\{\left(\frac{L+2}{L}\right)^2\frac{L+1}{L^2}\mathrm{sinc}^2\left(\frac{\pi m}{L}\right)\right.$$
$$\left.+\frac{2L+4}{L^2}\frac{1}{1+(m\pi/L)}+A(L)\right\}\sum_{i=1,i\neq k}^{M}\sum_{j=1,j\neq i}^{M}\left\{\frac{1}{2\sigma\sqrt{2\pi}}e^{-\frac{(f-2B_{rf}m-\Delta f_{ji})^2}{2\sigma^2}}\right. \quad \text{(A.15)}$$
$$\left.+\frac{1}{2\sigma\sqrt{2\pi}}e^{-\frac{(f-2B_{rf}m+\Delta f_{ji})^2}{2\sigma^2}}\right\}$$

At the output of the BPF, $N_{s_I-s_I}$ is given by

$$N_{s_I-s_I}=\left(\frac{\alpha P_s}{4}\right)^2\left\{\frac{1}{L^2}\left(\frac{L+2}{L}\right)^2+2\frac{L+2}{L}\overline{a_0^2}+\frac{1}{L}\right\}\sum_{i=1,i\neq k}^{M}\sum_{j=1,j\neq i}^{M}\Bigg[$$
$$erfc\left\{\frac{-2(f_{rf}+\Delta f_{ji})-B_{rf}}{2\sqrt{2}\sigma}\right\}-erfc\left\{\frac{-2(f_{rf}+\Delta f_{ji})+B_{rf}}{2\sqrt{2}\sigma}\right\}$$
$$+erfc\left\{\frac{-2(f_{rf}-\Delta f_{ji})-B_{rf}}{2\sqrt{2}\sigma}\right\}-erfc\left\{\frac{-2(f_{rf}-\Delta f_{ji})+B_{rf}}{2\sqrt{2}\sigma}\right\}\Bigg]. \quad \text{(A.16)}$$

The PDF of Δf_{ji}, $p(\Delta f_{ji})$, is given by

$$p(\Delta f_{ji})=\begin{cases}\frac{1}{(\Delta F)^2}(\Delta F-|\Delta f_{ji}|); \Delta f_{ji}\leq\Delta F\\ 0 \quad ;\Delta f_{ji}>\Delta F\end{cases}\quad (j,i=1,2,..,M;j,i\neq k;j\neq i). \quad \text{(A.17)}$$

The ensemble average of $N_{s_I-s_I}$, $\left\langle N_{s_I-s_I}\right\rangle$, is given by

$$\langle N_{s_I-s_I}\rangle=\int_{-\Delta F}^{\Delta F} N_{s_I-s_I} p(\Delta f_{ji})d\Delta f_{ji}. \tag{A.18}$$

Appendix B. Optical Signal Beat Noise for Fiber-Optic Radio Networks Using ROI-CDMA Method

We consider the optical beat noise caused by interferences between optical signals of a desired signal and an interference signal and between optical signals of two interference signals. Optical carrier signals of a desired signal from the j-th RBS at the upper and the lower ports of the k-th MZI, $f_{1j}(t)$ and $f_{2j}(t)$, can be written as

$$f_{1j}(t)=\left[P_s g_j(t)c_j(t).\frac{1+c_k(t)}{2}\right]^{1/2}\mathrm{Re}\left[e^{j\{2\pi f_{oj}t+\phi_j(t)}\right]\ j=1,2,..,M, \tag{B.1}$$

$$f_{2j}(t)=\left[P_s g_j(t)c_j(t).\frac{1-c_k(t)}{2}\right]^{1/2}\mathrm{Re}\left[e^{j\{2\pi f_{oj}t+\phi_j(t)+\pi\}}\right]j=1,2,..,M, \tag{B.2}$$

where f_{oj} is the center frequency of LD and $\phi_j(t)$ is the phase component of optical carrier at the j-th RBS. At first, we consider the beat noise between optical signals of a desired signal and an interference signal, $\langle N_{s_S-s_I}\rangle$.The current of beat noise between desired signal and interference at the input of BPF, $i_{s_S-s_I}(t)$, is given by

$$\begin{aligned} i_{s-s}(t)&=\sum_{j=1,j\neq k}^{M}\left[\frac{\alpha}{2}\left|f_{1k}(t)f_{1j}{}^{*}(t)\right|-\frac{\alpha}{2}\left|f_{2k}(t)f_{2j}{}^{*}(t)\right|\right]\\ &=\sum_{j=1,j\neq k}^{M}\frac{\alpha P_s}{2}\left[g_k(t)c_k(t)g_j(t)c_j(t)\right]^{1/2}\mathrm{Re}\left[e^{j\{2\pi\Delta f_{kj}t+\phi_k(t)-\phi_j(t)\}}\right].c_k(t), \end{aligned} \tag{B.3}$$

where $\Delta f_{kj}=f_{ok}-f_{oj}$. The autocorrelations of $c_k(t)$, $R_c(\tau)$, is given by [47]

$$R_c(\tau)=\frac{1}{L^2}+\frac{L+1}{L^2}\sum_{k=-\infty,k\neq 0}^{\infty}\mathrm{sinc}^2\left(\frac{\pi kT_c}{T_F}\right)\cos\left(\frac{2\pi k\tau}{T_F}\right). \tag{B.4}$$

The PSD of $c_k(t)$, $S_c(f)$, is given by

$$S_c(f)=\frac{1}{L^2}\delta(f)+\frac{L+1}{L^2}\sum_{m=-\infty,m\neq 0}^{\infty}\mathrm{sinc}^2\left(\frac{\pi m}{L}\right)\delta(f-2B_{rf}m). \tag{B.5}$$

It is assumed that the ROI-CDMA signal has a single mode gaussian shaped spectrum with the full width half maximum(FWHM) after ROI-CDMA driven by the biased bipolar, Δv, given by

$$\Delta\nu=\sqrt{\Delta\nu_{LD}+\left(LB_{rf}\right)^2}\,, \tag{B.6}$$

where $\Delta\nu_{LD}$ is the FWHM of the LD [6][15]. The PSD of $i_{sS-sI}(t)$, $S_{sS-sI}(f)$, can be written as

$$\begin{aligned} S_{sS-sI}(f)=\left(\alpha P_s\right)^2\frac{1}{L^2}\sum_{j=1,j\neq k}^{M}\left\{\frac{1}{2\sigma\sqrt{2\pi}}e^{-\frac{\left(f-\Delta f_{jk}\right)^2}{2\sigma^2}}\right. \\ \left.+\frac{1}{2\sigma\sqrt{2\pi}}e^{-\frac{\left(f+\Delta f_{jk}\right)^2}{2\sigma^2}}\right\}+\left(\alpha P_s\right)^2\frac{L+1}{L^2}\sum_{m=-\infty,m\neq 0}^{\infty}\operatorname{sinc}^2\left(\frac{\pi m}{L}\right) \\ \cdot\sum_{j=1,j\neq k}^{M}\left\{\frac{1}{2\sigma\sqrt{2\pi}}e^{-\frac{\left(f-2B_{rf}m-\Delta f_{jk}\right)^2}{2\sigma^2}}+\frac{1}{2\sigma\sqrt{2\pi}}e^{-\frac{\left(f-2B_{rf}m+\Delta f_{jk}\right)^2}{2\sigma^2}}\right\}, \end{aligned} \tag{B.7}$$

where

$$\sigma=\frac{\Delta\nu}{2\log 2} \tag{B.8}$$

The $S_{sS-sI}(f)$ appears in the radio frequency band after the photodetection, but its frequency location depends on the frequency difference among LD's of M RBS's. So we treat its power N_{sS-sI} as a random variable and derive its average power $\langle N_{sS-sI}\rangle$. At the output of the BPF, N_{sS-sI} is given by

$$\begin{aligned} N_{sS-sI}&=\left(\int_{-f_{rf}-B_{rf}/2}^{-f_{rf}+B_{rf}/2}+\int_{f_{rf}-B_{rf}/2}^{f_{rf}+B_{rf}/2}\right)S_{sS-sI}(f)df \\ &=\left(\alpha P_s\right)^2\frac{1}{L^2}\sum_{j=1,j\neq k}^{M}\left[erfc\left\{\frac{-2(f_{rf}+\Delta f_{jk})-B_{rf}}{2\sqrt{2}\sigma}\right\}\right. \\ &-erfc\left\{\frac{-2(f_{rf}+\Delta f_{jk})+B_{rf}}{2\sqrt{2}\sigma}\right\}+erfc\left\{\frac{-2(f_{rf}-\Delta f_{jk})-B_{rf}}{2\sqrt{2}\sigma}\right\}. \\ &\left.-erfc\left\{\frac{-2(f_{rf}-\Delta f_{jk})+B_{rf}}{2\sqrt{2}\sigma}\right\}\right] \end{aligned} \tag{B.9}$$

Assuming that optical carrier frequencies at RBS's, f_{oj} $(j=1,2,\ldots, M)$ are mutually independent random variables with its mean of f_0 and a uniform PDF in the range of $|f_{oj}-f_0|<\Delta F/2$ [6], the PDF of Δf_{kj}, $p(\Delta f_{kj})$, is given by

$$p(\Delta f_{kj})=\begin{cases}\dfrac{1}{(\Delta F)^2}(\Delta F-|\Delta f_{kj}|); \Delta f_{kj}\le \Delta F \\ 0 \qquad\qquad\qquad ; \Delta f_{kj}>\Delta F\end{cases} \quad (j,k=1,2,..,M, j\neq k). \tag{B.10}$$

The ensemble average of $N_{s_S-s_I}$, $\langle N_{s_S-s_I}\rangle$, is given by

$$\langle N_{s_S-s_I}\rangle=\int_{-\Delta F}^{\Delta F} N_{s_S-s_I}\, p(\Delta f_{kj})\, d\Delta f_{kj}. \tag{B.11}$$

The beat noise caused by an interference between optical signals of two interferences, $\langle N_{s_I-s_I}\rangle$ is examined. The current of beat noise between two interferences at the input of BPF, $i_{s_I-s_I}(t)$, is given by

$$\begin{aligned} i_{s_I-s_I}(t) &= \sum_{i=1,i\neq k}^{M}\sum_{j=1,j\neq i}^{M}\left[\frac{\alpha}{2}\left|f_{1j}(t)f_{1i}^{*}(t)\right|-\frac{\alpha}{2}\left|f_{2j}(t)f_{2i}^{*}(t)\right|\right] \\ &= \sum_{i=1,i\neq k}^{M}\sum_{j=1,j\neq i}^{M}\frac{\alpha P_s}{2}\left[g_i(t)c_i(t)g_j(t)c_j(t)\right]^{1/2}\mathrm{Re}\left[e^{j\{2\pi\Delta f_{ji}t+\phi_j(t)-\phi_i(t)\}}\right].c_k(t), \end{aligned} \tag{B.12}$$

where $\Delta f_{ji}=f_{oj}-f_{oi}$.

$$\begin{aligned} S_{s_I-s_I}(f)=&\left(\frac{\alpha P_S}{4}\right)^2\frac{1}{L^2}\sum_{i=1,i\neq k}^{M}\sum_{j=1,j\neq i}^{M}\left\{\frac{1}{2\sigma\sqrt{2\pi}}e^{-\frac{\left(f-\Delta f_{ji}\right)^2}{2\sigma^2}}\right. \\ &\left.+\frac{1}{2\sigma\sqrt{2\pi}}e^{-\frac{\left(f+\Delta f_{ji}\right)^2}{2\sigma^2}}\right\}+\left(\frac{\alpha P_S}{4}\right)^2\frac{L+1}{L^2}\sum_{m=-\infty,m\neq 0}^{\infty}\mathrm{sinc}^2\left(\frac{\pi m}{L}\right) \\ &\cdot\sum_{i=1,i\neq k}^{M}\sum_{j=1,j\neq i}^{M}\left\{\frac{1}{2\sigma\sqrt{2\pi}}e^{-\frac{\left(f-2B_{rf}m-\Delta f_{ji}\right)^2}{2\sigma^2}}\right. \\ &\left.+\frac{1}{2\sigma\sqrt{2\pi}}e^{-\frac{\left(f-2B_{rf}m+\Delta f_{ji}\right)^2}{2\sigma^2}}\right\} \end{aligned} \tag{B.13}$$

At the output of the BPF, $N_{s_I-s_I}$ is given by

$$N_{s_I-s_I}=(\int_{-f_{rf}-B_{rf}/2}^{-f_{rf}+B_{rf}/2}+\int_{f_{rf}-B_{rf}/2}^{f_{rf}+B_{rf}/2})S_{s_I-s_I}(f)df$$

$$=\left(\frac{\alpha P_S}{4}\right)^2\frac{1}{L^2}\sum_{j=1,j\neq k}^{M}\sum_{i=1,i\neq j}^{M}[$$

$$erfc\left\{\frac{-2(f_{rf}+\Delta f_{ji})-B_{rf}}{2\sqrt{2}\sigma}\right\}-erfc\left\{\frac{-2(f_{rf}+\Delta f_{ji})+B_{rf}}{2\sqrt{2}\sigma}\right\}. \tag{B.14}$$

$$+erfc\left\{\frac{-2(f_{rf}-\Delta f_{ji})-B_{rf}}{2\sqrt{2}\sigma}\right\}-erfc\left\{\frac{-2(f_{rf}-\Delta f_{ji})+B_{rf}}{2\sqrt{2}\sigma}\right\}]$$

The PDF of Δf_{ji}, $p(\Delta f_{ji})$, is given by

$$p(\Delta f_{ji})=\begin{cases}\frac{1}{(\Delta F)^2}(\Delta F-|\Delta f_{ji}|);\Delta f_{ji}\leq\Delta F\\ 0\quad ;\Delta f_{ji}>\Delta F\end{cases}(j,i=1,2,..,M;j,i\neq k). \tag{B.15}$$

The ensemble average of $N_{s_I-s_I}$, $\langle N_{s_I-s_I}\rangle$, is given by

$$\langle N_{s_I-s_I}\rangle=\int_{-\Delta F}^{\Delta F}N_{s_I-s_I}p(\Delta f_{ji})d\Delta f_{ji}. \tag{B.16}$$

Related Publications

[1] S.J. Park, K. Tsukamoto, and S. Komaki, "Proposal of direct optical switching CDMA for cable-to-the-air system and its performance analysis", IEICE Trans. on Commun. vol. E81-B, no.6, pp1188-1196, June 1998.

[2] S.J. Park, K. Tsukamoto, and S. Komaki, "Polarity-reversing type photonic receiving scheme for optical CDMA signal in radio highway", IEICE Trans. on Electron. vol. E81-C, no.3, pp462-467, March 1998.

[3] S.J. Park, K. Tsukamoto, and S. Komaki, "Multimedia mobile radio highway networks using optical CDMA multiplexing method", Proc. MDMC(Multidimensional Mobile Communications), Korea, pp.838-841, July 1996.

[4] S.J. Park, K. Tsukamoto, and S. Komaki, "Proposal of radio highway network using a novel Direct Optical Switched CDMA method", Proc. MWP(Microwave Photonics), TU4-6, Japan, pp.77-80, Dec. 1996.

[5] S.J. Park, K. Tsukamoto, and S. Komaki, "Radio highway networks using optical CDMA with optical polarity reversed correlator", Proc. MWP(Microwave Photonics), FR2-3, Germany, pp.227-230, Sep. 1997.

[6] S.J. Park, K. Tsukamoto, and S. Komaki, "Performance analysis of Direct Optical Switching CDMA Cable-To-The-Air network", Proc. SPIE(International Society for Optical Engineering) optical fiber communication, 3420-04, Taiwan, pp.20-29, Jul. 1998.

[7] S.J. Park, K. Tsukamoto, and S. Komaki, "Proposal of reversing optical intensity CDMA routing method in radio highway for CDMA radio", Proc. CIC(CDMA international conference), Korea, pp269-272, Oct. 1998.

[8] K. Tsukamoto, S. Fujii, S.J. Park, and S. Komaki, "Theoretical consideration on nonlinear distortion suppression in direct optical FM microwave over fiber system", Proc. MWP(Microwave Photonics), FR3-2, pp.251-255, Sep. 1997.

[9] K. Tsukamoto, S. Fujii, S.J. Park, and S. Komaki, " Fiber-optic microcellular communication system using frequency modulated LD and optical discriminator and its nonlinear distortion supersession", Proc. PIMRC(Personal Indoor and Mobile Radio Communications), pp.984-988, Sep. 1997.

[10] S. Fujii, S.J. Park, K. Tsukamoto and S. Komaki, "Proposal of compensation nonlinear scheme in optical direct FM fiber-optic microcellular communication system", Proc. OECC(Optoelectronics Communications), pp.312-313, Jul. 1998.

[11] K. Kumamoto, S.J. Park, K. Tsukamoto, and S. Komaki, " Higher-order bandpass sampling spreading scheme for direct optical switching CDMA radio highway", Proc. CPT(Contemporary Photonic Technologies), Jan. 1999.

[12] S.J. Park, K. Tsukamoto, and S. Komaki, "Proposal of radio highway networks using optical DOS-CDMA method", IEICE Tech. Report, OMI96-8, pp.39-44, July 1996.

[13] S.J. Park, K. Tsukamoto, and S. Komaki, "Theoretical analysis on connectable RBS number and CNR in direct optical switching CDMA radio highway", IEICE Tech. Report, MWP97-23, pp.80-85, Jan. 1998.

[14] S. Kajiya, S.J. Park, K. Tsukamoto, and S. Komaki, "A consideration on fiber-optic radio highway networks using CDMA method(II)", IEICE Tech. Report, RCS95-121, pp.63-68, Jan. 1996.

[15] S. Fujii, S.J. Park, K. Tsukamoto, and S. Komaki, "Theoretical performance analysis on direct optical FM radio highway and its nonlinear distortion suppression", IEICE Tech. Report, MWP97-6, pp.50-55, Oct. 1997.

[16] K. Kumamoto, S.J. Park, K. Tsukamoto, and S. Komaki, "A consideration on higher order bandpass sampling CDMA method for DOS-CDMA radio highway", IEICE Tech. Report, MWP98-32, OPE98-24, pp.53-60, June 1998.

[17] S. J. Park, K. Tsukamoto, and S. Komaki, "Proposal of CDMA cable-to-the-air system system", Proc. IEICE Spring Conf., SB-5-8, pp.665-666, Mar. 1996.

[18] S. J. Park, K. Tsukamoto, and S. Komaki, "Proposal of reversing optical intensity type DOS-CDMA radio highway", Proc. IEICE Autumn Conf., B-500, p.501, Sept. 1996.

[19] S. J. Fujii, S. Park, K. Tsukamoto, and S. Komaki, "Signal transmission performance

analysis of radio highway using direct optical frequency modulation", Proc. IEICE Spring Conf., B-5-260, p.647, Mar. 1997.

[20] K. Kumamoto, S.J. Park, K. Tsukamoto, and S. Komaki, "Proposal of aliasing canceller for DOS-CDMA radio highway", Proc. IEICE Spring Conf., B-5-262, p626, Mar. 1998.